https://doi.org/10.5194/acp-2022-228
Preprint. Discussion started: 1 April 2022

Atmospheric Chemistry and Physics Discussions

The simulation of mineral dust in the United Kingdom Earth System Model UKESM1.

Stephanie Woodward[1], Alistair A. Sellar[1], Yongming Tang[1], Marc Stringer[2], Andrew Yool[3], Eddy Robertson[1] and Andy Wiltshire[1].

[1]Met Office Hadley Centre, Exeter, UK
[2]Department of Meteorology, University of Reading, Reading, UK
[3]National Oceanography Centre, Southampton, UK

Correspondence to: Stephanie Woodward (stephanie.woodward@metoffice.gov.uk)

Abstract. Mineral dust plays an important role in earth system models, being linked to many components: atmospheric wind-speed, precipitation and radiation, surface vegetation cover and soil properties, and oceanic biogeochemical systems. In this paper the dust scheme in the first configuration of the United Kingdom Earth System Model UKESM1 is described, and simulations of dust and its radiative effects are presented and compared with results from the parallel coupled atmosphere-ocean general circulation model (GCM) HadGEM3-GC3.1. Not only changes in the driving model fields but also changes in the dust size distribution are shown to lead to considerable differences to the present-day dust simulations and to projected future changes. UKESM1 simulations produce a present-day top of the atmosphere (ToA) dust direct radiative effect (DRE - defined as the change in downward net flux directly due to the presence of dust) of 0.086 Wm^{-2} from a dust load of 19.5 Tg. Under climate change pathways these values decrease considerably: in the 2081–2100 mean of Shared Socioeconomic Pathway SSP5-8.45 ToA DRE reaches 0.048 W m^{-2} from a load of 15.1 Tg. In contrast, in HadGEM3-GC3.1 the present-day values of -0.296 W m^{-2} and 15.0 Tg are almost unchanged, at 0.289 W m^{-2} and 14.5 Tg in the 2081–2100 mean. The primary mechanism causing the differences in future dust projections is shown to be the vegetation response, which dominates over the direct effects of warming in our models. Though there are considerable uncertainties associated with any such estimates, the results presented demonstrate both the importance of the size distribution for dust modeling, and also the necessity of including earth system processes such as interactive vegetation in dust simulations for climate change studies.

https://doi.org/10.5194/acp-2022-228
Preprint. Discussion started: 1 April 2022

Atmospheric Chemistry and Physics Discussions

1 Introduction

Dust is an important component of the earth system being linked to the atmosphere, aerosols, surface, and terrestrial and oceanic biospheres (Carslaw et al., 2010). Many factors control the dust lifecycle, including vegetation cover, soil moisture, windspeed and precipitation; hence dust is potentially sensitive to changes in climate through multiple mechanisms. Dust, in turn, affects climate via radiative processes in the atmosphere, via interaction with clouds and other aerosol species, by changing surface albedo and as a source of nutrients for oceanic and terrestrial biogeochemical cycles.

Climate models have long included dust schemes (e.g. Tegen and Fung, 1994; Woodward, 2001; Miller et al., 2006; Kok et al., 2014), which typically allowed dust emission, transport and deposition to be modelled, together with the direct radiative effects of atmospheric dust. Some attempts were made to include the impact of the vegetation response on dust (Tegen et al., 2002; Mahowald et al., 2006), though as the vegetation was not simulated interactively, feedbacks between vegetation and climate were excluded. The advent of earth system models (Collins et al., 2011; Watanabe et al., 2011), which include interactive vegetation and ocean biogeochemical schemes together with other components, has extended the possibilities for the investigation of interactions between dust and other systems. This also allows for the impact of the responses of earth system components on the dust to be included in future climate projections.

Here we employ the state-of-the-art UKESM1 model (Sellar et al.,2019) to explore the behaviour of dust within the earth system in the present day and under possible future development pathways. UKESM1 is built around the HadGEM3-GC3.1 coupled ocean-atmosphere model (Kulbrodt et al., 2018; Williams et al., 2018), and we have made use of this to run parallel experiments with the coupled and earth system models, in order to investigate the importance of earth system processes to the dust simulation. Both models use the same dust emission scheme, though the tuning parameters were adjusted for UKESM1, as described in Seller et al (2019). We include particle sizes up to 63 μm diameter. Recent studies have suggested that the correct representation of super-coarse particles is important for the simulation of dust radiative effects (Ryder et al., 2019; Kok et al.,2017).

In this paper we give a brief introduction to UKESM1 and describe the dust scheme and the experiments used before assessing the present-day simulation of dust load, size distribution, aerosol optical depth (AOD) and deposition against observations, and we also present the simulated dust DRE results. We then compare UKESM1 and a set of HadGEM3-GC3.1 experiments in order to explore the relative importance of the various possible causes of differences between the two models, such as the size distribution, the additional earth system processes or the effects of re-tuning. In the next section we investigate the response of dust to potential climate change as driven by two Shared Socio-Economic Pathways and consider the mechanisms involved. Finally we present a discussion of the results and summarise our main findings.

2 UKESM1

UKESM1 is the latest generation UK earth system model built around the HadGEM3-GC3.1 coupled Atmosphere-Ocean GCM (Kulhbrodt et al., 2018; Williams et al., 2017) combined with the MEDUSA biogeochemical model (Yool et al.,

https://doi.org/10.5194/acp-2022-228
Preprint. Discussion started: 1 April 2022


Atmospheric Chemistry and Physics Discussions

2013). The interface between these is provided by the OASIS coupler (Craig et al., 2017). The component models within HadGEM3 are the Met Office Unified Model atmospheric model (UM) (Williams et al., 2018) containing the UKCA stratospheric-tropospheric chemistry (Archibald et al., 2020) and GLOMAP-mode aerosol (Mulcahy et al, 2020) schemes with earth surface model JULES (Walters et al., 2017) and the NEMO ocean and CICE sea-ice models (Storkey et al., 2018; Ridley et al, 2018). In UKESM1 these components are used for interactive simulation of earth system processes, such as the full atmospheric chemistry from UKCA. The modeling of vegetation and surface properties is particularly important for dust. In UKESM1 the TRIFFID scheme within JULES simulates interactive vegetation, whilst in HadGEM3-GC3.1 data from the IGBP climatology (IGBP, 2000) is used. The soil parameters also differ: those in HadGEM3-GC3.1 are based on Van Genuchten (Loveland et al., 2000), whilst those in UKESM1 are from Brooks and Corey (1964). A full description of UKESM1 is available in Sellar et al. (2019).

The mineral dust is simulated within HadGEM3 by the fully interactive dust scheme described below, which is called each atmospheric model timestep. The driving fields are calculated directly by the UM and JULES, and dust impacts the rest of the model through radiative interactions with the UM atmosphere and through input to the ocean biogeochemistry in MEDUSA. In the current configuration the dust is externally mixed with other aerosols.

3 Dust Scheme

3.1 Description of Dust Scheme

The dust scheme is a development of that described in Woodward (2001) with significant improvements to the emission scheme and newer refractive index data. Dust emission in six size bins with boundaries at 0.06324, 0.2, 0.6324, 2.0, 6.324, 20.0 and 63.24 μm diameter is calculated at each atmospheric model timestep (20 mins). Within each bin dV/d(log(r)) is assumed constant, where V is particle volume and r is particle radius, giving a sectional distribution of dV/d(log(r)). Horizontal flux is calculated over a wider size range, with three additional bins with boundaries at 63.24, 200.0, 632.4 and 2000.0 μm diameter.

Flux calculations are based on the method of Marticorena and Bergametti (1995). Horizonal flux in bin i is given by:

$$G_i = \rho\, B\, U^{*3} (1+U^*_{ti}/U^*)\ (1-(U^*_{ti}/U^*)^2)\, M_i\, C\, D / g \quad (1)$$

where ρ is surface air density, B is bare soil fraction, U^*_{ti} is threshold friction velocity for the bin, U* is friction velocity excluding orographic effects, C is a constant of proportionality set to 2.61 from wind-tunnel experiments, D is a tuneable parameter and g is acceleration due to gravity. M_i is the mass fraction of particles in the bin, obtained from soil clay, silt and sand fractions from HWSD data (Nachtergaele et al., 2008) according to the method described in Woodward (2001).

In UKESM1 dust is emitted only from the bare soil fraction of a gridbox, though there is also an option in the code to allow emissions from seasonally bare sources, based on the leaf area index (LAI). Dust emissions are inhibited if snow is present, if the ground is frozen, on steep slopes, if soil moisture exceeds a threshold (see below) and at coastal points where the lowest level windspeed over land may be anomalously high. No preferential source terms are used.

https://doi.org/10.5194/acp-2022-228
Preprint. Discussion started: 1 April 2022


Atmospheric Chemistry and Physics Discussions

The driving fields for the scheme are the model's grid-box mean, time-step mean fields, but equation (1) was derived from instantaneous measurements at single locations. Corrections are therefore needed to account for the effect of spatial and temporal averaging. Here, model friction velocity U^*_M is multiplied by a dimensionless tuneable constant k_1.

$$U^* = k_1 U^*_M \quad (2)$$

The value of k_1 was chosen empirically, as described in section 3.3.

Dry threshold friction velocity (U^*_{td}) values were obtained from Bagnold (1941). The effect of soil moisture on friction velocity is represented using the method of Fécan et al. (1999), which has been shown to agree well with measurements. Threshold friction velocity for moist soil is related to the dry threshold friction velocity by:

$$U^*_t/U^*_{td} = 1 \quad \text{for } w<w'$$

$$U^*_t/U^*_{td} = (1 + 1.21(w-w')^{0.68})^{0.5} \quad \text{for } w>w' \quad (3)$$

where $w'=0.14 F_C^2 + 17.0 F_C$

F_C is clay fraction and w is volumetric soil moisture. The model provides average soil moisture over the 10 cm deep top soil level (w_1). In order to obtain soil moisture near the surface, as well as to correct for the effects of temporal and spatial averaging, the model soil moisture is multiplied by a dimensionless tunable constant k_2:

$$w = k_2 w_1 \quad (4)$$

The highest clay fraction reported in the measurements on which the algorithm was based was 0.2 (Gillette, 1979). However, it subsequently became clear that the single measurement with this high clay fraction was contaminated by upstream dust (Gillette, pers. Comm., reported in Alfaro and Gomes, 2001). The next highest clay fraction measured was 0.1. As high clay fractions result in unrealistically high emissions from the dust scheme, a maximum of 0.1 is applied, with higher values of F_C being reset to this.

The Fécan et al. treatment of soil moisture was designed for use in arid or semi-arid areas, and in order to apply it to the whole earth, a further constraint on dust production from moist soil is required. Dust production is inhibited when soil moisture exceeds a particle-size dependent threshold (w_t), which was chosen to correspond approximately to the maximum soil moisture for which movement was detected in the observations used by Fécan et al..

$$w_t = (F_C + 0.12) / 0.03 \quad (5)$$

The vertical dust flux is calculated for six bins in the range 0.06324 to 63.24 μm, corresponding to the smallest six horizonal flux bins. Total vertical flux relates to total horizontal flux summed across all bins according to the method of Marticorena and Bergametti (1995), which is based on the measurement data of Gillette (1979). The size distribution across the six vertical flux bins follows that of the equivalent horizontal flux bins. Vertical flux in bin i (F_i), for i=1 to 6 is given by:

$$F_i = 10^{(13.4\, Fc - 6.0)}\ G_i\ \Sigma_{i=1,9}(G_i) / \Sigma_{i=1,6}(G_i) \quad (6)$$

Dust is transported as 6 independent tracers corresponding to the 6 vertical flux bins. Deposition through below-cloud scavenging, turbulent mixing and sedimentation is included, as described in Woodward (2001). The radiative effects of dust on the atmosphere are simulated with the model's 2–stream radiation code (Edwards and Slingo, 1996). Dust radiative properties were derived from the data of Balkanski (2007) for Saharan dust. This is intended to provide the optimum

https://doi.org/10.5194/acp-2022-228
Preprint. Discussion started: 1 April 2022


Atmospheric Chemistry and Physics Discussions

simulation of dust from the Sahara, the world's largest dust source, though the radiative effects of dust from other sources with other mineralogical contents will inevitably be less well modelled (Sokolik and Toon, 1999). In UKESM1 the total marine dust deposition flux is passed into the ocean, where it is used by the MEDUSA ocean biogeochemical scheme (Yool et al., 2013) as a source of iron for plankton growth.

The scheme described here uses the same code as the UM global atmosphere GA7.1 and global coupled GC3.1 configurations, but with two changes in the settings: 1) the three tuning terms (D, k_1 and k_2) are different and 2) the emission of dust from seasonally vegetated sources which is allowed in GA7 and GC3.1 is deactivated in UKESM1. The latter was done both because it was unclear whether the simulation of the global distribution of the various plant types would be sufficiently accurate for the purpose, and also because the JULES land surface tiling on which the seasonal source code depends had been changed for UKESM1, rendering the associated dust settings invalid. Seasonal sources accounted for less than 10% of the load in HadGEM3-GC3.1, so this was not expected to have a large impact.

3.2 Diagnostics

The model provides a self-consistent set of diagnostics of dust emissions, depositions and mixing ratios (concentrations). Whilst the concentration, wet deposition, and dry deposition over water are directly comparable to results from other models and to observations, the emission and dry deposition in source regions are not. Atmospheric lifetime, being derived from these terms, is also not comparable. The emission and dry deposition diagnostics include all particles released from the surface, whether or not they are added to the atmospheric load or interact with the model atmosphere in any way. In the Unified Model the flux of particles released from the surface is calculated first and then another section of code performs both the mixing into the atmosphere and the dry deposition back to the surface in a single loop. As a result, a fraction of the particles released from the surface is immediately dry-deposited and never added to the atmospheric burden. In physical terms the re-deposited fraction may be considered as those particles which fall back to the surface within the model timestep. The magnitude of this effect is greater for larger particles due to the size-dependence of sedimentation; and because the particle size range extends to 63 μm it has a considerable impact on the total emission and deposition diagnostics, and also the calculated lifetime.

3.3 Dust Tuning

The values of the parameters D, k_1 and k_2 above were obtained empirically. Sets of UKESM1 experiments were run with different values of the parameters, and the simulation was compared with observations of near-surface dust concentrations, AODS, dust size distribution and observation–derived deposition rates. Initial sets of tuning experiments were used to explore the parameter space, finding how the model responded to changes in each of the variables and constraining their range; later experiments focussed on finer tuning of the variables. Due to time constraints much of this work was carried out in parallel with the last stages of UKESM1 development, so ongoing adjustments had to be made to the tuning terms in response to changes in the ESM. Though otherwise not ideal, this parallel development had the advantage that minor

https://doi.org/10.5194/acp-2022-228
Preprint. Discussion started: 1 April 2022


Atmospheric Chemistry and Physics Discussions

changes could be made to other parts of the ESM to improve the dust simulation. In particular, the lai_min term for grasses in JULES was reduced to 0.3, allowing the grasses to spread more readily and improving the simulation of bare soil fraction (Sellar et al., 2019) . The final parameter values chosen were $D=1.0 \times 10^{-3}$, $k_1=1.1$,$k_2=0.8$. It is likely that had further time been available these values would have been adjusted slightly to optimise the results further. The corresponding HadGEM3-GC3.1 values were $D=2.25\times10^{-4}$, $k_1=1.45$, $k_2=0.5$.

The tuning was carried out primarily with UKESM1-CN, the off-line chemistry version of UKESM1 (Sellar et al., 2019) as this ran more quickly than the full UKESM1 and the interactive chemistry was expected to have little impact on the dust. Comparisons of dust simulations from the two versions of the ESM showed only small differences, with the various tuning settings tending to perform similarly in each case. Pre-industrial (PI) simulations were used for the tuning as a fully spun-up present-day experiment was not available at that stage. Whilst this meant that the model climate did not match the period of the observations, this discrepancy was likely to have had a relatively small effect compared with the cumulative effect of the many uncertainties in the dust scheme, such as biases in the simulated bare soil fraction, soil moisture and wind-speed, resolution-related limitations in capturing some emissions mechanisms, and the omission of surface-crusting effects and other poorly understood processes. Tuning tests were also carried out with "pseudo-present-day" experiments, initialised from PI runs, but then run to equilibrium with present-day (PD) atmosphere and land-use settings. These produced similar results to the main tuning experiments and gave confidence in the use of PI simulations to establish tuning parameters.

4 Experiments

Name	Model	Parallel CMIP6 Experiment	Meaning period	Tuning Settings D,k_1,k_2	Seasonal Sources
UK_PI	UKESM1	piControl	20 yrs	(UKESM1)	(off)
H3_PI	HadGEM3-GC3.1	piControl	20 yrs	(HadGEM3_GC3.1)	(on)
H3_PD	HadGEM3-GC3.1	Historical	1995-2014	(HadGEM3_GC3.1)	(on)
UK_PD	UKESM1	Historical	1995-2014	(UKESM1)	(off)
H3_TUK_EXSS	HadGEM3-GC3.1	Historical	1995-2014	UKESM1	off
H3_TUK_INSS	HadGEM3-GC3.1	Historical	1995-2014	UKESM1	(on)
UK_S5	UKESM1	SSP5-8.5	2081-2100	(UKESM1)	(off)
H3_S5	HadGEM3-GC3.1	SSP5-8.5	2081-2100	(HadGEM3_GC3.1)	(on)
UK_S2	UKESM1	SSP2-4.5	2081-2100	(UKESM1)	(off)
H3_S2	HadGEM3-GC3.1	SSP2-4.5	2081-2100	(HadGEM3_GC3.1)	(on)
A_UK_PI	HadGEM3-GA7.0	piClim-control	30 yrs	UKESM1	off
A_UK_PI_V2014NOLU	HadGEM3-GA7.0	piClim-histNoLU	30 yrs	UKESM1	off

Table 1: Summary of experiments. The UKESM1 tuning settings for D,k_1 and k_2 are $1.0\text{x}10^{-3}$, 1.1 and 0.8 respectively; the HadGEM3 settings are $2.25\text{x}10^{-4}$,1.45,1.1. Tuning Settings and Seasonal Source settings in brackets indicate that the values are the usual ones for the model used in that experiment. For further explanation of these terms see Section 3.

https://doi.org/10.5194/acp-2022-228
Preprint. Discussion started: 1 April 2022


Atmospheric Chemistry and Physics Discussions

The results presented here were primarily obtained from UKESM1 and HadGEM3-GC3.1 historical experiments parallel to those performed as part of CMIP6 (Eyring et al., 2016), but with extra diagnostics. In order to obtain diagnostics needed for calculating DRE, a copy of each relevant CMIP6 experiment was run for 20 years with the "double call" method. This involved calling the radiation scheme twice each timestep, with the radiative effect of dust excluded from the first call but included in the second which is used to progress the model. The dust DREs are then calculated as the differences between the fluxes from each call. In addition, two parallel HadGEM3-GC3.1 experiments were run: in both of these the tuning terms were set to UKESM1 values, and in one the seasonal sources were also deactivated. These allowed us to investigate the relative importance of the various differences between the main simulations. Two UKESM1 AMIP experiments from CMIP6 were also used. The experiments are summarised in Table 1.

5 Present-day dust simulations and evaluation

5.1 Concentration and load

Figure 1 shows dust load from the UKESM1 and HadGEM3-GC3.1 present-day simulations (UK_PD and H3_PD), together with the differences and fractional differences. Whilst both models capture the expected global dust distributions qualitatively well, the global load in UK_PD is 30% higher than in H3_PD. The UK_PD load of 19.5 Tg is in good agreement with the AeroCom mean of 19.2Tg (Textor et al, 2006).

https://doi.org/10.5194/acp-2022-228
Preprint. Discussion started: 1 April 2022

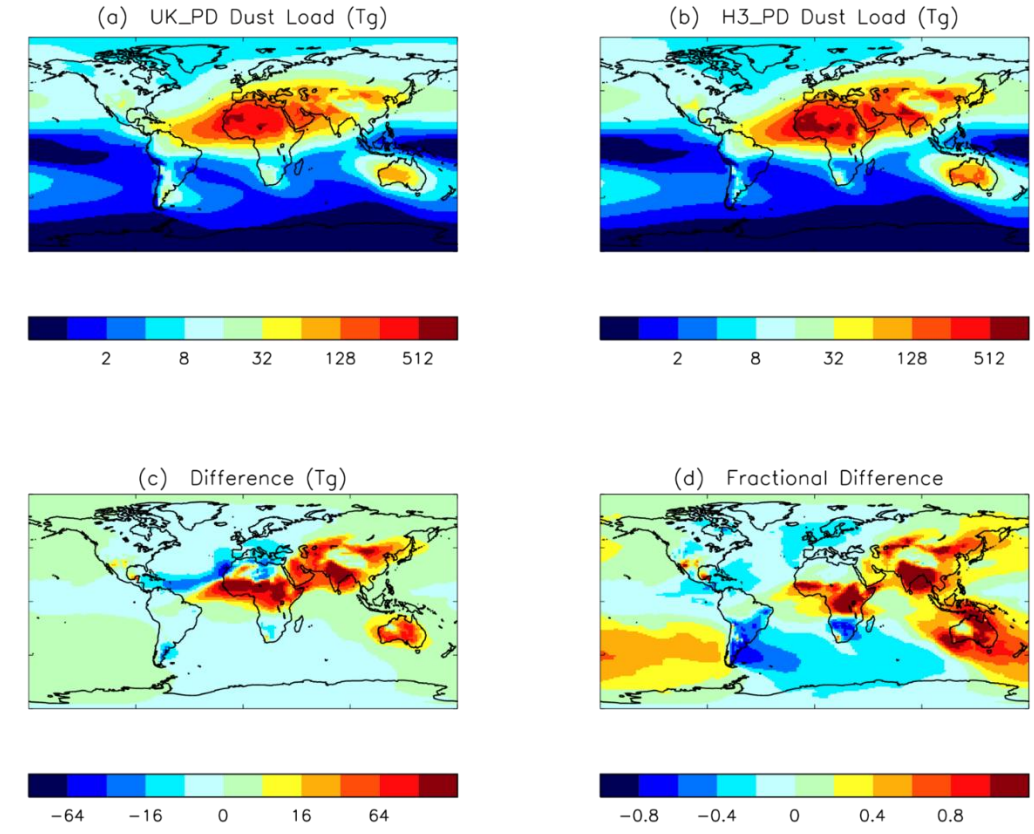

Figure 1: Dust load (Tg) from H3_PD and UK_PD, difference and fractional difference.

Figure 2 shows scatterplots of seasonal mean modelled dust concentrations versus observations from remote sites from the University of Miami network and dust-dominated AERONET (Holben et al., 2001) sites. At least four years of monthly data was available for the chosen sites. Both UK_PD and H3_PD show good agreement with the observations, with the models being within a factor of three of the observations at most stations for most seasons. The slight high bias at a few North Pacific stations in spring and summer is increased in UKESM1 due to larger bare soil areas in Asia simulated by TRIFFID, with associated increased windspeed and reduced soil moisture. Similarly, increased bare soil in Australia results in an increased high bias at the nearest South Pacific station. The low biases almost all occur at two stations on the Antarctic Peninsula, where the dust from Patagonia dominates. The concentrations here are likely to be very sensitive to the westerly winds in that region, and the position of the Subtropical Front. The bias is worsened in UKESM1 due to a low bias in the simulated bare soil fraction. Overall, the UKESM1 surface concentrations show good agreement with observations, compared with other ESMs (Checa-Garcia et al, 2021). The similarity in the level of performance between UKESM1 and

https://doi.org/10.5194/acp-2022-228
Preprint. Discussion started: 1 April 2022

Atmospheric Chemistry and Physics Discussions

HadGEM3-GC3.1 is noteworthy, given the many extra processes and feedbacks within the ESM, and in particular its use of interactive vegetation.

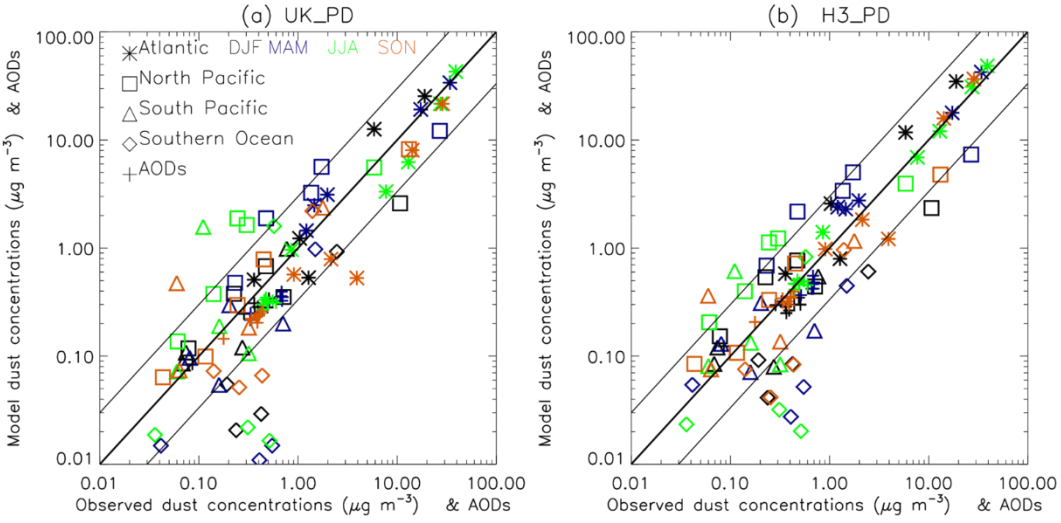

Figure 2: Scatterplots of model versus observational multi-annual seasonal mean concentrations at remote marine locations and AODs in dusty areas for (a) UK_PD and (b) H3_PD. Near-surface concentrations are from the University of Miami Network, and AoDs from AERONET vn3.

5.2 Size distribution

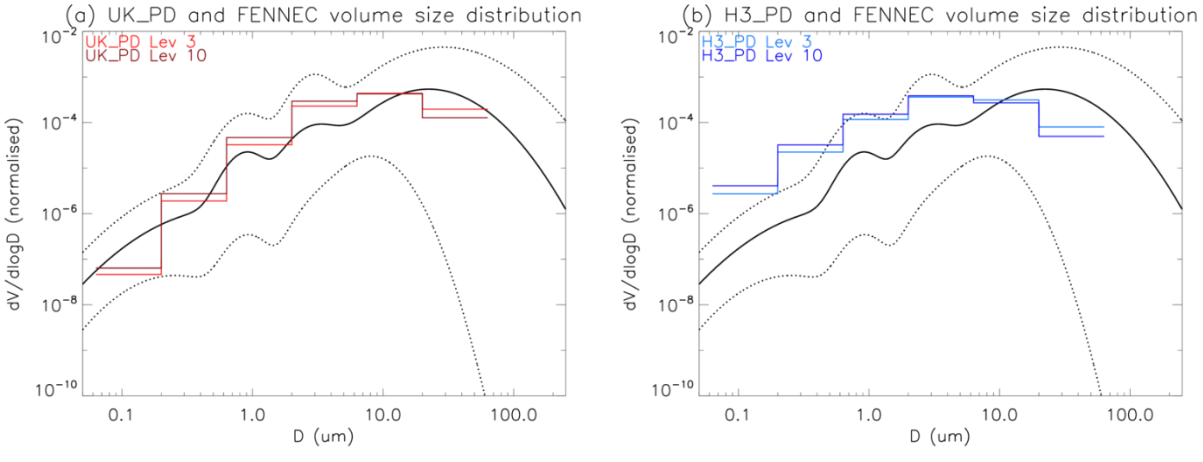

Figure 3: Normalised volume size distribution from a fit to FENNEC mean, maximum and minimum data (Ryder,2013) with (a) UK_PD and (b) H3_PD. Model data is a multi-annual June mean from a rectangular area 13W-4W, 21S-26N which covers the

https://doi.org/10.5194/acp-2022-228
Preprint. Discussion started: 1 April 2022


Atmospheric Chemistry and Physics Discussions

FENNEC campaign region. Data from model levels 3 (approx. 96m) and 10 (approx. 770m) correspond to the height range of most of the FENNEC measurements.

225 UKESM1 dust was tuned to give better agreement with the size distribution data from the FENNEC campaign (Ryder et al., 2013) than was shown in HadGEM3-GC3.1. This data was particularly useful as it provided measurements near sources where the effects of deposition and transport on the size distribution would be relatively small, and, unusually, it included data from several instruments for measuring larger particles with diameters above 3μm. The FENNEC campaign took place in June 2011 in the remote Sahara.

230 Figure 3 presents normalised volume size distributions from 20 year June means from UK_PD and H3_PD compared with a fit to the FENNEC observations. UK_PD shows good agreement with the observations throughout the size range.. The lower level data has a somewhat greater coarse particle fraction than the higher level data, as might be expected in a source region, given the short lifetimes of the largest particles. The peak dimeter is slightly smaller than in the observations. This would be consistent with the 20 year June mean containing a smaller fraction of freshly emitted particles than were measured

235 in observations which were intended to sample dusty conditions.

H3_PD concentrations overlap with the FENNEC observations, though the overall agreement is poorer as the model is outside the range of the observations for the two smallest bins and the peak of the distribution is in bin 4 (2–6 μm diameter), rather below the peak diameter of the observations.

5.3 Optical depth

240 Comparison of monthly mean model AODs with data from AERONET (Holben et al.,2001) sites in dusty areas (Fig. 4) shows that the modest low bias in H3_PD is slightly worsened in UK_PD, though the model mean is within 2 standard deviations of the observations in almost all cases. The stations were selected to obtain as realistic observational climate means as possible given the considerable variability of dust and the short data record, and to minimise the effects of other aerosols. Sites were chosen from those in potentially dusty areas, as having a minimum of 4 years of monthly data with at

245 least 10 daily means per month, and a monthly mean Angstrom exponent (870 - 440) below 0.5 for at least 10 months of the year. The only sites to fulfil these criteria were: Tamanrasset_INM in the Sahara, Capo Verde off the west African coast and six Sahelian stations all in a narrow band between 12° and 16° north.

https://doi.org/10.5194/acp-2022-228
Preprint. Discussion started: 1 April 2022

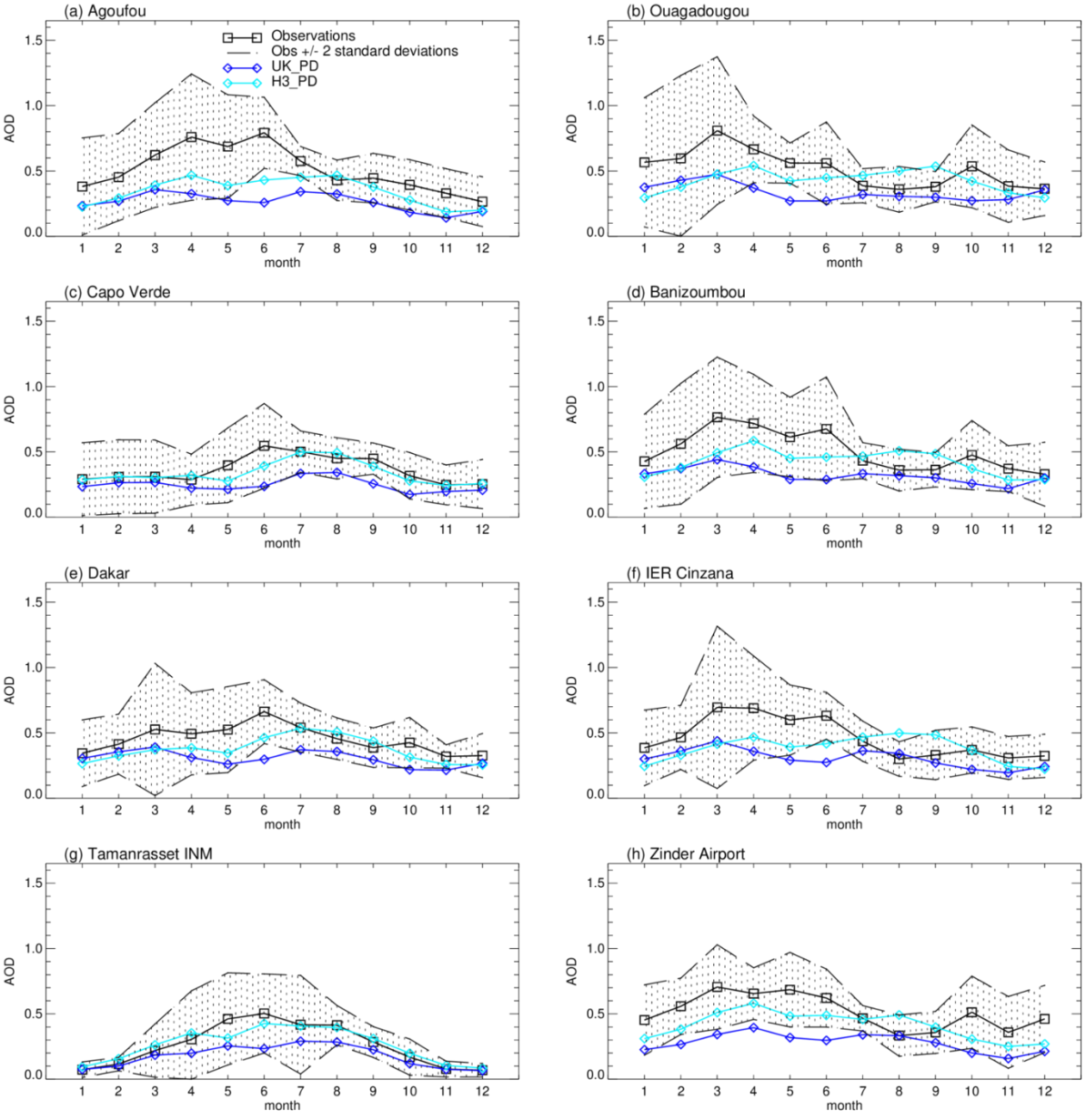

Figure 4: Annual cycle of AOD (440nm) at dust-dominated AERONET stations.from UK_PD and H3_PD. Site locations: Agoufou [1.48W,15.35N], Oagadougou [1.40W, 12.20N], Capo Verde [22.94W,16.73N], Banizoumbou [2.66E, 13.54N], Dakar [19.96W, 14.39N], IER Cinzana [5.93W, 13.28N], Tamanrasset INM [5.53E, 22.79N], Zinder airport [8.99E, 13.78N].

Studies by Marticorena et al. (2010, 2017) have shown that the annual cycle of dust in the western Sahel is related to the timing of the West African Monsoon (WAM) and the annual north-south shift in the ITCZ. Through winter and early spring the Harmattan flow brings dust from the Sahara to this region, and the increasing AODs over the first few months of the year

https://doi.org/10.5194/acp-2022-228
Preprint. Discussion started: 1 April 2022


Atmospheric Chemistry and Physics Discussions

are consistent with the annual cycle of Saharan dust, as seen at Tamanrasset-INM. From May to October the WAM dominates the region, bringing precipitation and winds from the southwest. During the early part of the monsoon season strong but sporadic local emission events driven by Mesoscale Convective Systems (MCS) produce similar levels of dust to those seen in the dry season. The UK_PD simulations slightly underestimate the AODs due to Saharan dust in the dry season, but the main sources of error appear to be in the timing of the arrival of the WAM, with AODs already decreasing in April, and in particular a failure to simulate the dust production from local sources. These failings are unsurprising, given the difficulties in simulating the WAM and MCS in an N96 climate model (Marsham et al.,2011; Heinold et al., 2013) and in simulating realistic vegetation cover in this marginal area. In this regard, the performance at Sahelian sites cannot be considered representative of the dust simulation generally.

At Tammanraset UKESM1 simulates the dry season dust well, but underestimates the wet season AOD. The AOD at Capo Verde is dominated by Saharan dust, and shows similar patterns. Guiardo et al (2014) identify four source areas for Tamanrasset: dust from an area immediately south of the site and from the east Libyan desert affects the site all year, whilst dust from the western Sahara and the Libya-Tunis border only reach Tamanrasset in the wet season. Some of these areas could be affected by errors in the simulation of the WAM and the position of the ITCZ; windspeed bias could also be involved, as could resolution-related issues such as difficulties in the simulation of Low Level Jets or the representation of local orography, as well as biases in the dust scheme.

Figure 5, which compares the total aerosol optical depth at 550nm in UK_PD with MODIS data shows a low bias in the Sahel as mentioned above, and also in dust from the Bodele depression. The Bodele dust source is very difficult to simulate in global climate models because a resolution of a few 10s of km is needed to represent the Bodele Low Level Jet, which is responsible for much of the dust emissions (Todd et al., 2007). The dust-dominated AOD over the northern Sahara and the Arabian Peninsula is also low, whilst over Australia it is too high. The high bias on the southwest side of the Himalayas and low bias on the northeast side suggest the model may be failing to transport aerosol over the steep orography there. These biases reflect model weaknesses and also the difficulty of finding a single set of tuning terms which gives a good performance against all metrics: settings which gave improvement in AOD over North Africa resulted in worsening of biases associated with Asian and Australian dust.

The effects of non-sphericity on dust particle optical properties were not included in the models. It has been estimated that the extinction efficiency could increase by as much as 29% (Kok et al., 2017). An indication of the potential effect this might have was estimated by multiplying the UK_PD dust optical depth by a factor of 1.29, which resulted in improved agreement with the satellite data (Fig. 5).

https://doi.org/10.5194/acp-2022-228
Preprint. Discussion started: 1 April 2022

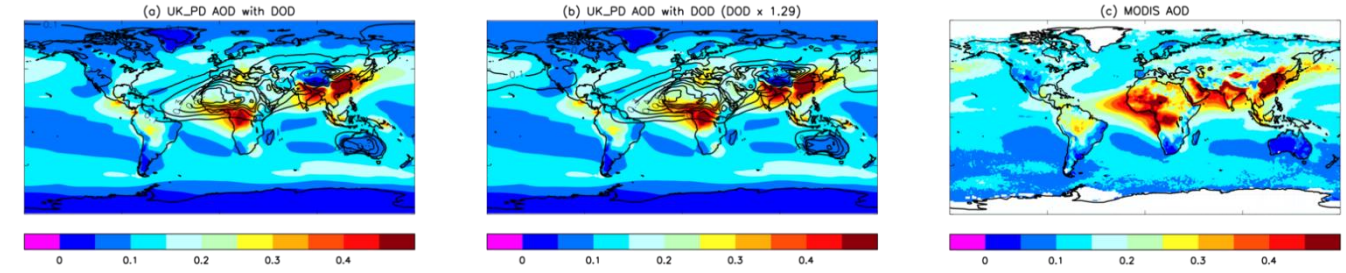

Figure 5: AOD (550nm) from (a) UK_PD, with contours showing the fractional contribution of dust to total AOD; (b) as (a) but with dust optical depth multiplied by 1.29; (c) MODIS 2003-2012 mean.

290

5.4 Deposition

Though the model deposition diagnostics will not represent observed deposition in source regions (see above), they are comparable to measurements in locations where there are no local emissions. Deposition rates have been evaluated against annual mean measured fluxes from a range of data sources at sites remote from emission areas, as selected by Huneeus et al. (2011) for the evaluation of dust in AeroCom models. These include deposition observations from Ginoux at al. (2001), dust and iron deposition fluxes reported in Mahowald et al. (2009), ice core data from Mahowald et al (1999) and sediment trap data from the DIRTMAP database (Tegen et al., 2002; Kohfeld and Harrison, 2001). Though this collection of deposition data from 84 sites is one of the most comprehensive available, there are considerable uncertainties associated with the observations: most notably that, although sites with less than 50 days of data were excluded, some of the records are not long enough to be considered climatological (Huneeus, 2011). This is particularly problematic for dust fields which show very strong variability: a large fraction of annual deposition may occur over a few days of the year (Prospero et al.,2010).

A scatterplot of UK_PD mean deposition rates against these observation (Fig. 6) shows that the model agrees reasonably well with the observations, and model results are within a factor of 10 of the observations at most locations. The only area with a noticeable bias is in Antarctica and the Southern Ocean. The four Antarctic stations where the model significantly overestimates deposition rates are very close together near Dumont station, between 64.60–64.97S and 141.07–141.45E. This localised bias may be due to overestimates in windspeed or in sea-ice cover and hence roughness. Superficially, the results appear broadly comparable to those of the AeroCom models reported in Huneeus et al.(2010), though those data represent the output of models run for a single year, in most cases with winds derived from re-analyses. UKESM1 deposition rates also compare well to those of other ESMs in the CRESCENDO project, as recorded by Checa-Garcia et al. (2021).

https://doi.org/10.5194/acp-2022-228
Preprint. Discussion started: 1 April 2022

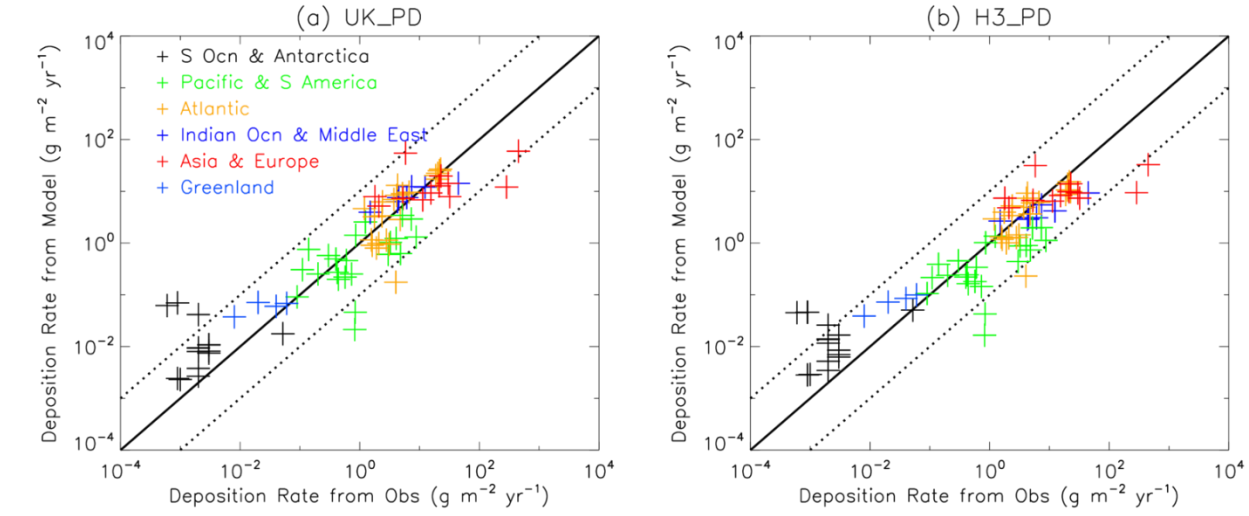

Figure 6: Scatterplot of deposition rates (g m-2 yr-1) from UK_PD and H3_PD vs observations (Huneeus, 2011)

5.5 Radiative effects

Figure 7 and Table 2 show the dust direct radiative effect (DRE) - the change in flux directly due to the presence of dust, excluding any secondary effects. This is calculated using the "double call" method as described in Section 4.

In UKESM1 dust is generally more reflective than the surface in the shortwave (SW) , except over ice and the brightest deserts, with the results that the net downward shortwave at the top of the atmosphere (ToA) is reduced everywhere but over these very light surfaces. The global mean ToA SW dust DRE is -0.280 W m^{-2}, and -0.410 W m^{-2} in the clearsky (CS). The ToA longwave (LW) DRE is positive everywhere with a global mean of 0.194 W m^{-2} (0.237 W m^{-2} CS). These combine to give a positive net DRE over the Sahara, but partially cancel in most other regions to produce modest positive net values over lighter surfaces and negative net values elsewhere, giving a global mean of only -0.086 W m^{-2}. At the surface the global mean net DRE is -0.168 W m^{-2}, being positive over the brightest surfaces and negative elsewhere. The surface SW DRE is negative everywhere and has a global mean of -0.556 W m^{-2} (-0.679 W m^{-2} CS); the LW is positive everywhere, with a global mean of 0.388 W m^{-2} (0.455 W m^{-2} CS).

In HaGEM3-GC3.1 the dust shortwave effect is larger and the longwave effect smaller. This is associated with the difference in size distribution between the UK_PD and H3_PD simulations, as will be explored in Section 5.6.

The relatively small global mean net DREs are the residuals of the partial cancellation of areas of larger positive and negative net DREs, as well as the partial cancellation of component DREs of different sign, each of which are sensitive to changes in the dust load, spatial distribution, size distribution and radiative properties. As a result, there are large uncertainties associated with estimates of global mean dust DREs

https://doi.org/10.5194/acp-2022-228
Preprint. Discussion started: 1 April 2022

Atmospheric Chemistry and Physics Discussions

Experiment	Load (Tg)	ToA SW (W m^{-2})	ToA LW (W m^{-2})	ToA Net (W m^{-2})	Surf.SW (W m^{-2})	Surf. LW (W m^{-2})	Surf. Net (W m^{-2})
H3_PD	15.01	-0.460	+0.164	-0.296	-0.688	+0.338	-0.350
diff due to tuning (size distribution)	-	+0.276 -60%	-0.021 -13%	+0.255 -86%	+0.288 -42%	-0.026 -8%	+0.262 -75%
H3_TUK_INSS_NL	15.01	-0.184	+0.143	-0.041	-0.400	+0.312	-0.088
diff due to tuning (load)	-4.63 -31%	+0.057 -31%	-0.044 -31%	+0.013 -31%	+0.123 -31%	-0.096 -31%	+0.027 -31%
H3_TUK_INSS	10.38	-0.127	+0.099	-0.028	-0.277	+0.216	-0.061
diff due to seasonal sources	-0.98 -9%	+0.011 -9%	-0.009 -9%	-0.002 -9%	-0.027 -10%	-0.020 -9%	+0.007 -12%
H3_TUK_EXSS	9.40	-0.116	+0.090	-0.026	-0.249	+0.196	-0.053
diff due to driving model	+10.14 +108%	-0.164 +141%	+0.103 +115%	-0.061 +236%	-0.307 +123%	+0.192 +98%	-0.115 +215%
UK_PD	19.54	-0.280	+0.194	-0.086	-0.556	+0.388	-0.168
diff from H3_PD to UK_PD	+4.52 +30%	-0.180 -39%	-0.030 +18%	-0.210 -71%	-0.132 -19%	-0.049 +15%	-0.182 -52%

335

Table 2: Global mean load and all-sky direct radiative effects due to dust in a present-day climate, from various experiments. Alternate rows show experimental results and the absolute and percentage differences between the experiment below and the experiment above

https://doi.org/10.5194/acp-2022-228
Preprint. Discussion started: 1 April 2022

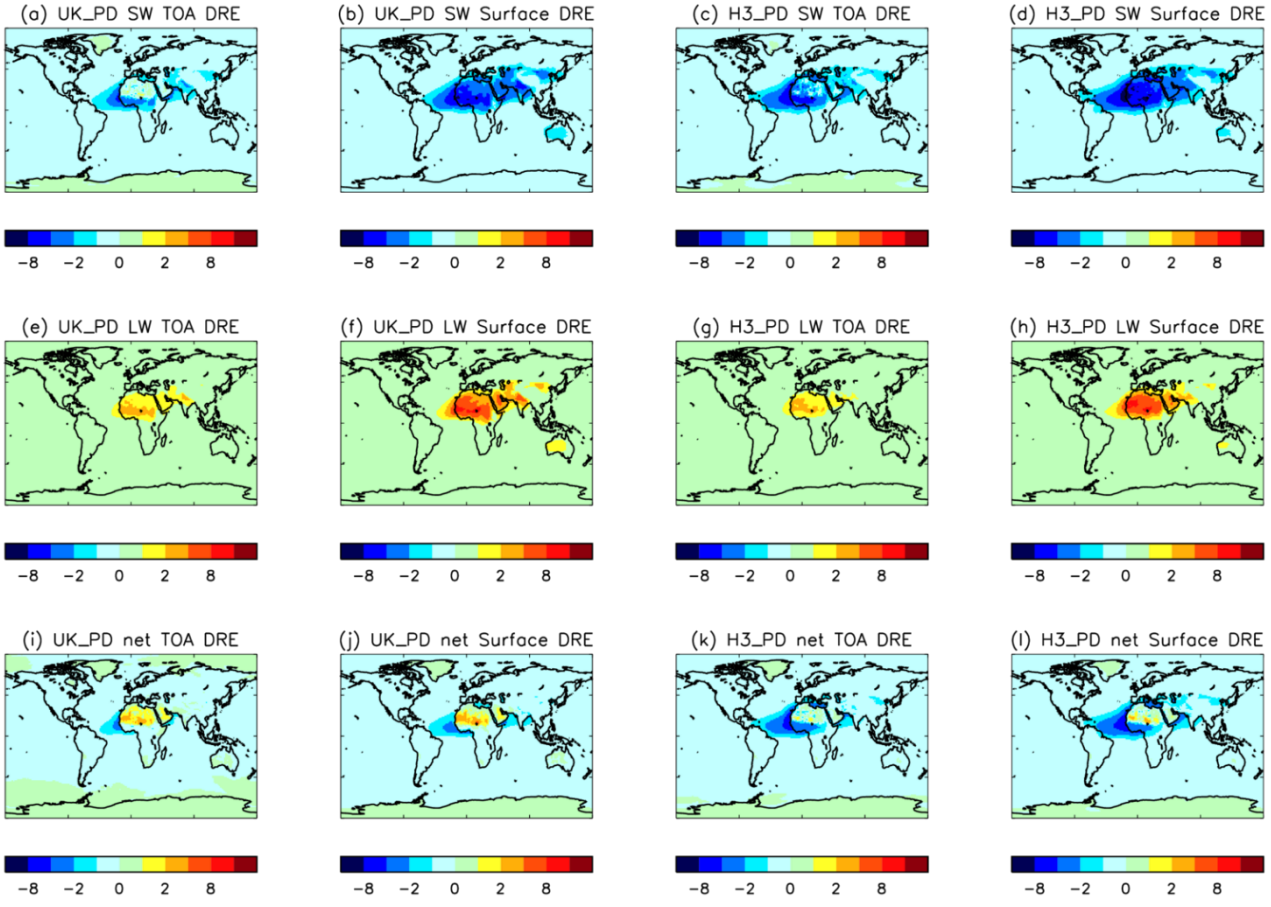

Figure 7: Dust direct radiative effects (Wm^{-2}) in UK_PD and H3_PD.

5.6 Drivers of UKESM1 – HadGEM3-GC3.1 differences

Running simulations with almost identical dust schemes in two similar models allows us to explore the impacts of a number of factors on the dust simulation. The causes of the differences between the HadGEM3-GC3.1 and UKESM1 present-day dust load and DREs may be divided into four groups: 1) The change in size distribution with re-tuning; 2) The change in total load due to re-tuning; 3) The (de-)activation of seasonal sources; and 4) The change of driving model. These are investigated using results from H3_PD, UK_PD and two additional experiments representing intermediate configurations. H3_TUK_EXSS is a HadGEM3-GC3.1 experiment with UKESM1 dust tuning and excluding seasonal sources, to help isolate the effects of the change in model. H3_TUK_INSS is parallel to this but includes seasonal sources to allow investigation of the effect of these sources (see Table 1). Another set of dust DRE results H3_TUK_INSS_NL have been generated by normalising the DREs from H3_TUK_INSS by the ratio of H3_PD load to H3_TUK_INSS load. This allows

https://doi.org/10.5194/acp-2022-228
Preprint. Discussion started: 1 April 2022


Atmospheric Chemistry and Physics Discussions

us to separate the effects of the change in size distribution (from comparing H3_TUK_INSS_NL and H3_PD) from the effects of the load change (from comparing H3_TUK_INSS_NL and H3_TUK_INSS). The implicit assumption that the DREs are proportional to total load for a given size distribution is a reasonable first approximation, although it ignores the feedback between dust DREs and emissions (Woodage and Woodward, 2014; Kok et al., 2018). Load and DREs from each experiment are listed in Table 2.

The changes from H3_PD to UK_PD result in an increase in total load of 30%. The load change due to re-tuning (Factor 2) is responsible for a reduction of 31%, whilst the disabling of seasonal sources (Factor 3) only decreases global mean load by a further 9%. The change in driving model (Factor 4) more than doubles the load, which is much the largest individual impact on load, indicating the importance of including earth system processes in dust simulations. This increase is mainly due to the larger bare-soil source area simulated by TRIFFID in UKESM1 compared with the IGBP climatology in HadGEM3-GC3.1. Where vegetation cover is lost, not only is a larger area susceptible to deflation but surface wind-speed increases, and enhanced evaporation leads to reduced soil moisture, all of which tend to increase dust emissions, as illustrated in Figure 8.

Global mean dust net DREs in UKESM1 are smaller than in HadGEM3_GC3.1, despite the larger load (Table 2, Fig. 7). The net surface DRE of -0.168 W m^{-2} is about half the H3_PD value of -0.350 W m^{-2}, and the -0.086 W m^{-2} net ToA DRE is less than one third of the H3_PD value of -0.296 W m^{-2}. These global means are the residuals of the partial cancellation of SW and LW DREs, as well as of spatial meaning of areas of net DRE with different signs. Change in size distribution is the factor which produces the largest absolute change in the net DREs, due to its large impact in the SW not being balanced by its much smaller LW effect: SW DREs are approximately halved due to the size distribution change, mainly because of reductions in the load of finer particles in bins 2 and 3 (0.2–2.0 μm); whilst LW DREs are only reduced by about 10%, chiefly because the reduction in the load of coarser particles is relatively small. Under the change in size distribution, the global load of bin 4 particles (2.0–6.3 μm), which dominate the LW effect, is almost unchanged, with increases in the Saharan plume and northern mid-latitudes balanced by reductions elsewhere; and the numbers of bin 5 and 6 particles (6.3–63 μm), which are somewhat less radiatively active, are increased at the expense of the smaller bins which dominate the SW

https://doi.org/10.5194/acp-2022-228
Preprint. Discussion started: 1 April 2022

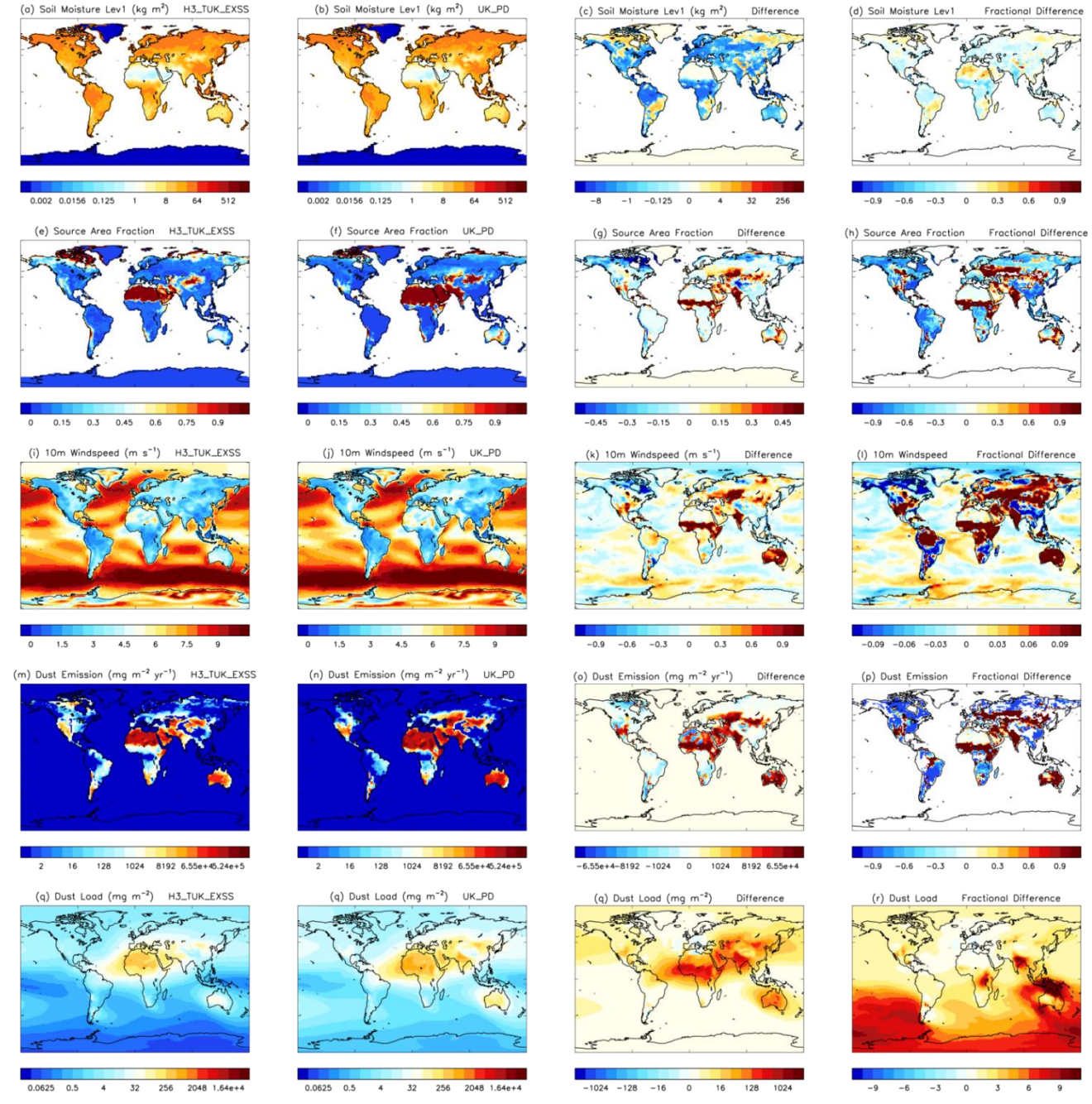

Figure 8: Soil moisture in top model layer, dust source area fraction, 10m wind-speed, dust emission diagnostic and dust load from H3_TUK_EXSS and UK_PD, and the differences and fractional differences between experiments.

https://doi.org/10.5194/acp-2022-228
Preprint. Discussion started: 1 April 2022


Atmospheric Chemistry and Physics Discussions

6 The response of dust to changing climate

The global mean pre-industrial to present-day dust forcing (defined here as the change in DRE) is small in both models. It is calculated as the difference between dust DREs in the 20 year mean UK_PD (and H3_PD) runs, and a 20 year mean from the respective PI control runs. UKESM1 (HadGEM3-GC3.1) simulates a forcing of +0.007 W m^{-2} (-0.029 W m^{-2}) at ToA and +0.005 W m^{-2} (-0.038 W m^{-2}) at the surface, from a change in dust load of -0.099 Tg (+1.400 Tg).

The role of the vegetation response in the historical dust changes is investigated using the results of atmosphere only AMIP experiments in which the driving fields, except vegetation, were taken from a UKESM1 pre-industrial simulation. In the control experiment (A_UK_PI) the vegetation fields - LAI, canopy height and vegetation fraction - were also taken from the pre-industrial simulation; in the parallel A_UK_PI_V2014NOLU experiment the 2014 vegetation values from a UKESM1 historical experiment which excluded anthropogenic land-use changes were used. In both experiments the dust settings were as in UKESM1. The difference between these simulations gives an estimate of the effect of the change in vegetation alone on dust. The effect of climate change excluding the vegetation response (but including land-use change) is estimated from the difference between HadGEM3-GC3.1 simulations H3_PD and H3_PI.

Figure 9 shows the differences in dust load due to vegetation response and to climate estimated in this way, together with the sum of these two changes, and the equivalent change in UKESM1 from the pre-industrial UK_PI to the present-day UK_PD. The similarities between the patterns of load change due to the combined vegetation and climate changes and due to the changes in UKESM1 is notable, giving confidence that dust changes simulated by the models are comparable even though the present-day dust is somewhat different. From these experiments the global totals of the PD to PI differences in dust load are -1.04 Tg due to the vegetation response, +1.40 Tg due to climate (and land-use) change and -0.10 Tg due to all the processes in UKESM1. The difference between the UKESM1 PI to PD changes and the sum of the vegetation and climate driven changes is caused by a combination of the interactions of earth system processes, the differences between the dust settings in HadGEM3-GC3.1 and UKESM1, and the natural variability of dust. In our models, the impact of the vegetation response on dust was comparable in magnitude but opposite in sign to the direct impact of climate change over the historical period

The dust changes due to possible future changes in climate are explored using a set of scenario experiments representing future Shared Socio-Economic Pathways (Sellar et al., 2020; Riahi et al., 2017). Means of the last 20 years (2081-2100) of SSP5-8.5 and SSP2-4.5 experiments UK_S5, H3_S5, UK_S2 and H3_S2 are compared with the present day (1995-2014) period of the historical experiments UK_PD and H3_PD. The Shared Socio-Economic Pathway SSP5-8.5 represents high-end projections of fossil fuel and energy use, food demand and greenhouse gas emissions, assuming fossil-fuelled development; it has a radiative forcing pathway similar to the highest Representative Concentration Pathway RCP8.5 (Moss et al., 2010; van Vuuren et al., 2011). SSP2-4.5 represents a “Middle of the Road” future, with social, economic and technological developments broadly following historical patterns, giving a radiative forcing pathway similar to RCP4.5. The scenario experiments are initialised from the end of the respective historical runs.

https://doi.org/10.5194/acp-2022-228
Preprint. Discussion started: 1 April 2022

Atmospheric Chemistry and Physics Discussions

415

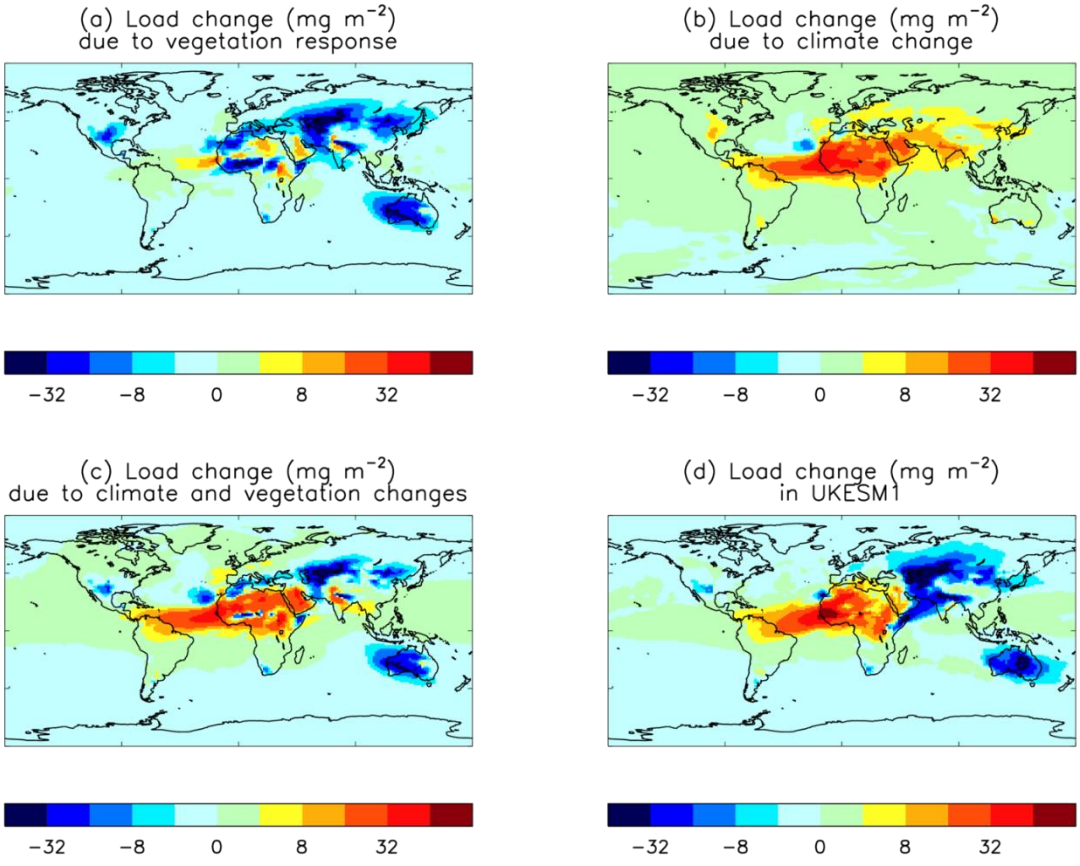

Figure 9: Difference in dust load (mg m-2) from pre-industrial to the present day due to changes in vegetation (from A_UK_PI_V2014 – A_UK_PI) , due to changes in climate and land-use (from H3_PD – H3_PI), the sum of these two (A_UK_PI_ V2014 – A_UK_PI)+ (H3_PD – H3_PI), and in the full earth system model (from UK_PD – UK_PI).

420

Results are summarised in Table 3. UKESM1 simulates a reduction of 23% in total dust load from the present day to the end of the SSP5 scenario, with the greatest reductions from the major deserts, and only small areas experiencing increases (Fig. 10). In contrast the global load in HadGEM3-GC3.1 decreases by only 4%, with smaller local changes than in UKESM1 and reduced emissions from some deserts almost completely balanced by increases elsewhere (Fig. 11). The equivalent
425 results for SSP2-4.5 are reductions of 19% for UKESM1 and 7% for HadGEM3-GC3.1. In each model the pattern of load changes from the present to the end of SSP2-4.5 have very similar geographical distribution to the equivalent SSP5-8.5 results. This is also true of the main drivers of dust emissions: soil moisture, source areas and windspeed. The slightly larger decrease in dust load in H3_S2 compared with H3_S5 is due to minor differences in the residuals from the

https://doi.org/10.5194/acp-2022-228
Preprint. Discussion started: 1 April 2022


Atmospheric Chemistry and Physics Discussions

cancellation of areas of positive and negative change. Given the similarities in the patterns of change of dust and its drivers in both pathways, the following analysis will focus only on the SSP5-8.5 experiments.

Experiment	Source Area Fraction	Load (Tg)	ToA SW (W m^{-2})	ToA LW (W m^{-2})	ToA Net (W m^{-2})	Surface SW (W m^{-2})	Surface LW (W m^{-2})	Surface Net (W m^{-2})
H3_PD	0.458	15.01	-0.460	+0.164	-0.296	-0.688	+0.338	-0.350
H3_S2	0.486	13.95						
H3_S5	0.485	14.47	-0.440	+0.150	-0.289	-0.652	+0.291	-0.361
UK_PD	0.255	19.54	-0.280	+0.194	-0.086	-0.556	+0.388	-0.168
UK_S2	0.237	15.74						
UK_S5	0.221	15.07	-0.191	+0.143	-0.048	-0.400	+0.269	-0.132

Table 3: Dust source area fraction, atmospheric load and DRE from simulations of present-day and future climates. (NB DRE diagnostics were not available for the H3_S2 and UK_S2 experiments.)

Comparison of the changes in the drivers of dust emissions helps reveal the causes of the differences between the dust changes in the two models. Figures 10 and 11 show the changes in vegetation, dust source areas, soil moisture, windspeed and dust from the present day to the SSP5-8.5 future simulations in UKESM1 and HadGEM3-GC3.1 respectively. In UKESM1 the dynamic vegetation responds to the warming climate and enhanced CO2 by producing increased growth. Areas of bare soil are colonised by grasses, whilst existing grassland is taken over by shrubs and trees. Land-use changes produce the opposite effect: areas of trees are lost to crops (grasses), most notably in sub-Saharan Africa, though this effect is small compared to the climate-driven vegetation changes. The net result is a decrease in bare soil, particularly in mid-latitudes. HadGEM3-GC3.1 vegetation only includes the land-use changes, which are represented as changes to the Tree, Shrub and Grass plant functional types. The bare soil fraction is constant, though source areas do show systematic change as dust is produced from seasonally vegetated grass and shrub areas in that model.

The top-level soil moisture in UKESM1 is reduced in all areas except deserts, giving a global mean loss of 12%. A similar reduction of 15% is seen in HadGEM3-GC3.1 suggesting that this effect is mostly a response to the changing climate, mediated by evaporation and somewhat mitigated by the reduction in bare soil fraction in the earth system model.

In UKESM1 the lowest-level windspeed over land is reduced in northern mid- and high-latitudes as well as in Australia and southern South America, but is increased in parts of the tropics, particularly tropical South America, though not in desert regions. HadGEM3-GC3.1 exhibits similar increases in the tropics, but the mid- and high-latitude reductions are much smaller. This indicates that the tropical increases in windspeed are likely to be primarily a response to the changing climate, whilst the reductions likely are due to increased roughness produced by vegetation growth in the corresponding areas in UKESM1.

https://doi.org/10.5194/acp-2022-228
Preprint. Discussion started: 1 April 2022


Atmospheric Chemistry and Physics Discussions

The increase in dust emissions at high latitudes in HadGEM3 is driven predominantly by the reduction in soil moisture and at low latitudes by the increases in windspeed, whilst the reduced emissions from arid areas are caused by the slightly reduced windspeeds and moister soil in those regions. These processes also occur in UKESM1, but the vegetation driven loss of bare soil and larger reduction in windspeed have a greater impact, resulting in enhanced reduction of emissions, with emissions increases occurring in only a few small regions. Whilst there is a global near balance of dust load increases and decreases in HadGEM3-GC3, UKESM1 simulates a global load reduction of 23% by the end of SSP5-8.5.

The difference in dust responses between the models is much larger than the difference in dust responses between the pathways. HadGEM3-GC3.1 results suggest that the global dust burden dust will remain largely unchanged whatever socio-economic pathway is followed, with increases mostly in North and South America and Australia balanced by decreases mainly in North Africa, Asia and Europe. In contrast, in UKESM1 the addition of the extra earth-system process, and particularly the interactive vegetation, results in projections of reduced global total load, with reductions from most of the main desert regions and only a few small areas of increase in the tropics. The global load reduction of 23% associated with "Fossil-fuelled development" is somewhat larger than the 19% reduction of the "Middle of the road" pathway. Our simulations suggest that the impact of the vegetation response on dust is larger than the direct impact of future climate change; and the differences due to including earth system processes in the simulations is larger than the differences between pathways.

The reduction in load in UKESM1 results in a decrease in ToA DRE from UK_PD to UK_SP5 of 44%, though the absolute values are small (-0.086 and -0.048 W m^{-2}). The H3_S5 global mean TOA DRE of -0.29 W m^{-2} is only 2% greater than the H3_PD value. In UKESM1 in particular, local changes are much larger than the global mean (Fig. 7).

https://doi.org/10.5194/acp-2022-228
Preprint. Discussion started: 1 April 2022

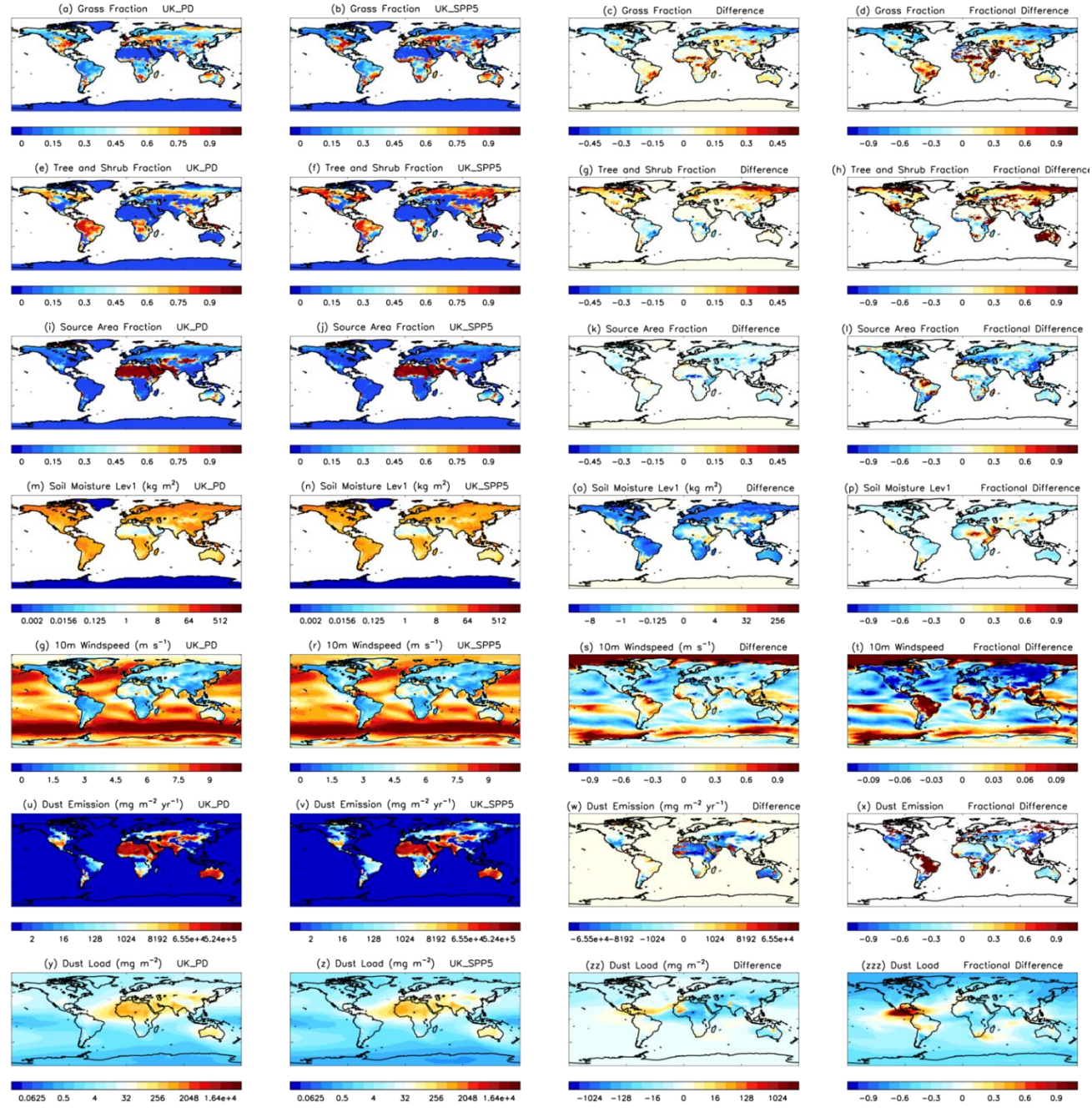

Figure 10: Grass fraction, tree and shrub fraction, dust source area fraction, soil moisture in top layer, 10m windspeed, dust emission diagnostic and dust load from UK_PD and UK_SSP5, together with differences and fractional differences between experiments.

https://doi.org/10.5194/acp-2022-228
Preprint. Discussion started: 1 April 2022

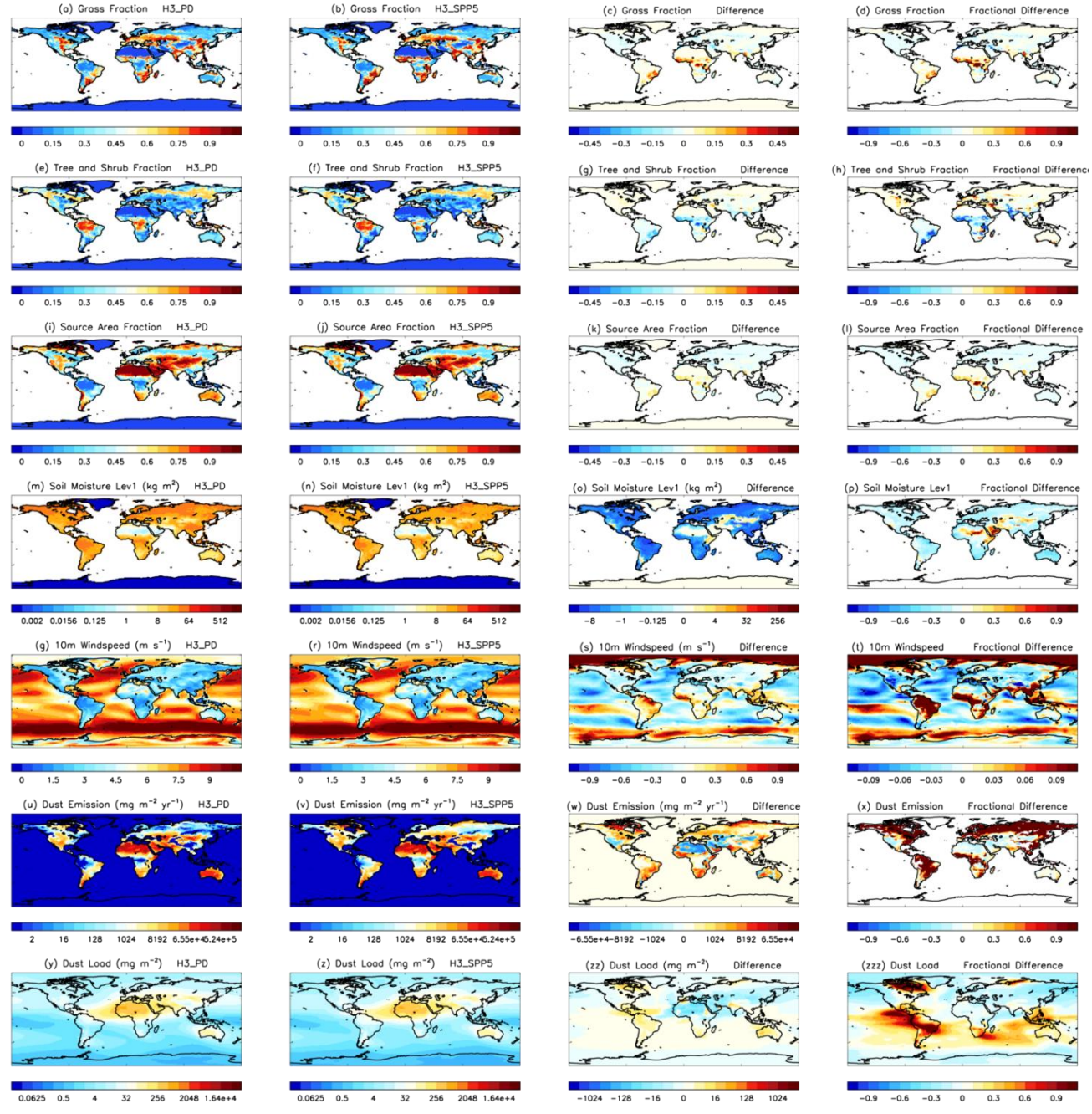

Figure 11: as Fig. 10 but for H3_PD and H3_SSP5.

https://doi.org/10.5194/acp-2022-228
Preprint. Discussion started: 1 April 2022


Atmospheric Chemistry and Physics Discussions

7 Discussion

The simulation of present-day dust in UKESM1 shows good agreement with most of the observations, though AoD is somewhat low. The performance is comparable with that of HadGEM3_GC3.1, despite the extra complexity of the additional processes and feedbacks in the earth system model. Some degradation in model performance is to be expected as a cost of this increased complexity, which is included to allow investigation of the feedback processes (Jones et al., 2011). Despite this, it was not found necessary to limit dust emissions by imposing any sort of preferential source terms, so the dust was able to respond to climate-driven changes without any potentially unrealistic constraints. The tuning of the lai_min term for grasses in JULES, which limits the rate at which grasses can spread, was an important factor in this, as it improved the simulation of bare soil fraction. Dust is particularly sensitive to the interactively simulated vegetation in an earth system model, because where vegetation is lost not only do source areas increase, but the consequent reduced roughness and enhanced evaporation lead to increased windspeed and reduced soil moisture respectively, all of which changes tend to increase dust emissions

The results demonstrate the crucial role of the particle size distribution in the simulation of the 3D dust distribution and particularly the radiative effects. Comparison of H3_PD with H3_TUK_INSS_NL (and H3_TUK_INSS) shows that quite small shifts in the size distribution towards coarser particles can change the balance of global mean SW and LW DREs so that they almost completely balance, giving net DREs close to zero The particle size range is the same in all cases, with a maximum diameter of 63μm, which is larger than many other climate model dust schemes (Huneeus et al, 2011; Checa-Garcia et al, 2012), so the DREs from HadGEM3-GC3.1 already include a relatively large LW effect, and hence relatively small net DREs.

The DRE results from UKESM1 are consistent with the estimates of Kok et al (2017), who find that most models underestimate the size of atmospheric dust compared with measurements, and use analysis of size and other observations to constrain model estimates of dust ToA DRE to a range between -0.48 W m^{-2} and +0.2 W m^{-2}. This compares with a range of results from -0.56 W m^{-2} to +0.01 W m^{-2} reported in Forster et al. (2007), and more recent studies have also fallen within the latter range (Miller et al., 2006; Balkanski et al., 2007, Mahowald et al.,06; Albani et al., 2014), though Scanza et al. (2015) have a slightly more positive ToA DRE of +0.05 W m^{-2}. Note that a small net ToA DRE does not necessarily imply a minimal effect on climate. Even globally homogeneous LW–SW compensation has been shown to affect climate (Tilmes et al., 2016), and in the case of dust regional effects will be important.

The response of dust to climate change in each of the models is very different, predominantly due to the direct and indirect impacts of the vegetation changes in UKESM1 which are not included in HadGEM3-GC3.1. This suggests that in the future the main anthropogenic impact on dust may be via the change in vegetation consequent on fossil-fuel driven emissions rather than through the changes in climate variables, whilst changes in land-use have a smaller effect. The differences between the models are greater than the differences between the SSP2 and SSP5 simulations from either model. These results illustrate

https://doi.org/10.5194/acp-2022-228
Preprint. Discussion started: 1 April 2022


Atmospheric Chemistry and Physics Discussions

the importance of including earth system processes when simulating the response of dust to climate change: indeed a realistic future dust simulation may not be possible without including vegetation changes and its effects.

A feature of the pattern of emission changes, particularly in UKESM1, is the location of areas of large increase very close to areas of large decrease, with a sharp boundary between them. This demonstrates the sensitivity of the dust to the balance of the various driving fields, as well as the high sensitivity to windspeed. Even modest biases in driving model fields could produce shifts in such balances, and the areas of sharp gradients in dust changes are unlikely to be captured correctly by any current schemes and present a challenge for future dust modeling.

As is often the case with the development of a model which includes dust, our tuning of the dust in the final UKESM1 configuration was limited by time constraints, and further work might result in an alternative choice of alternative choice of settings. For example, in the UKESM1.1 model configuration dust was re-tuned to give better agreement with observations of AODs, though at the expense of agreement with other observations of size distribution and concentrations in some areas (Mulcahy et al., 2022). The main weakness of the UKESM1 settings is the low bias in AoD in the Saharan plume, which depends on dust optical properties as well as size distribution and concentrations. The properties are based on observations, but may well not be representative for all Saharan dust. In particular, dust from the Bodele is made up predominantly of diatomite, which has different physical properties compared with dust from other Saharan sources (Todd et al., 2007). The size distribution was shown to agree well with observations. Up to half the dust emissions from West Africa may be associated with cold pool outflows from moist convection (haboobs), but the parametrised rather than explicit convection in the model renders the simulation of these events very difficult (Marsham et al., 2011; Knippertz and Todd, 2012), likely leading to underestimation of emissions in that area. Emissions from the Sahel are probably also underestimated for similar reasons. The omission of dust ageing has the effect of increasing dust concentrations remotely from sources and though this is not a very large effect, the inclusion of ageing could impact the choice of tuning settings, allowing higher Saharan AoDs without too much over-estimation of concentrations in other areas. A higher present-day AoD over the Sahara would likely be associated with larger DREs in both the SW and LW, assuming the size distribution was unchanged. These would still largely cancel, but the net DRE would probably be larger, as would the projected forcings for 2100.

Some uncertainties are inevitably associated with any such dust simulations as these. Lack of observational input data, such as global surface geomorphology, limits dust simulations; and some processes, such as dry and wet deposition, are also only poorly constrained by observations. Schemes may lack some processes – for example, the ageing of dust particles is omitted here – and simplifications such as using a single set of refractive index data for all dust are almost unavoidable at present. The driving models also have limitations which affect the dust simulation. The strong dependence of emissions on friction velocity renders the dust particularly sensitive to biases in wind speeds. The ability of a vegetation scheme to simulate the global distribution of bare source areas is also critical for dust emissions. For this work we chose not to include emissions from seasonal sources because they depend on the distributions of various plant types, and it was not clear whether these could be simulated with sufficient realism. There is also a paucity of good quality data for evaluation of global dust simulations on climatological timescales. Despite such factors, the results of experiments such as these can provide much

https://doi.org/10.5194/acp-2022-228
Preprint. Discussion started: 1 April 2022


Atmospheric Chemistry and Physics Discussions

useful information, so long as the limitations are borne in mind. Further work is required to provide the missing observations, to study the processes affecting dust, and to improve dust schemes and the models driving them, in order to enhance understanding and improve the simulation of the effects of climate change on dust.

8 Conclusions

The dust scheme used in UKESM1 and HadGEM3-GC3.1 is a development of the Woodward (2001) scheme with an improved emissions parametrisation. It was initially used in HadGEM3 and then re-tuned for UKESM1. Seasonal sources were also de-activated in UKESM1, reducing dependence on multiple plant types in the interactive vegetation scheme whilst having only a small effect on load (less than 10% in HadGEM3-GC3.1). Evaluation of the UKESM1 present-day dust simulation showed good agreement with observations, comparable with that of HadGEM3-GC3.1. This is particularly encouraging given the additional uncertainties produced by the extra processes and feedbacks within the earth system model, and the fact that no preferential source terms were used in either model.

The differences between global mean UKESM1 and HadGEM3-GC3.1 present-day DREs have been shown to depend on the change in size distribution consequent on re-tuning as much as on the change in driving model. The change in load due to re-tuning had a lesser impact, and the activation of seasonal sources produced only a small effect. This demonstrates the importance of the simulation of size distribution, which impacts the global dust concentrations through the size dependent deposition processes and additionally impacts DREs through the size dependent radiative properties. The magnitude of this effect will depend on the choice of refractive index data.

The response of the dust under future socio-economic pathways is highly model dependent. In HadGEM3-GC3.1 the climate response produces drying of moist soils which tends to increase emissions slightly, but this is balanced by a small reduction in windspeeds in major source regions leading to the total emissions and load remaining almost unchanged between the present day and 2100. Whilst these processes also occur in UKESM1, a greater impact on dust comes from the vegetation response, which is simulated interactively in this model. Enhanced vegetation growth produces a decrease in bare soil leading to further reductions in windspeed, both of which result in lower emissions and load. The differences between the models are greater than the differences between the SSP2-4.5 and SSP5-8.5 pathways and, though there are some considerable uncertainties associated with these results, they indicate the importance of including the vegetation response in projections of dust in future climates.

These results provide useful new information about the interactions between dust and climate. They highlight the need to represent the full dust size distribution as realistically as possible, and indicate that the effect of doing this may be to reduce the global mean net dust DREs at ToA to a value close to zero (though impacts on climate may be larger, particularly on a regional scale). They also show the importance of including earth system interactions in dust simulations over climate timescales, as the greatest driver of dust change may be vegetation changes and the consequent modifications to source areas, soil moisture and windspeed.

https://doi.org/10.5194/acp-2022-228
Preprint. Discussion started: 1 April 2022

Code Availability.

Information on the UKESM1 configuration and its components and the pre-requisites for using it may be found at http://cms.ncas.ac.uk/wiki/UM/Configurations/UKESM (last access 12 Mar 2022). Due to intellectual property rights we cannot provide the source code or documentation papers for the UM or JULES. A number of national meteorological services and research organisations use the UM in collaboration with the Met Office to undertake research, produce forecasts, develop the UM code and build and evaluate Earth system models. The UM is available for use in this way under licence; see http://www.metoffice.gov.uk/research/modeling-systems/unified-model (last access 12 March 2022). JULES is available under licence free of charge for research purposes; see https://jules-lsm.github.io/access_req/JULES_access.html (last access 12 Mar 2022).

Data Availability.

The simulations used in this work are based on CMIP6 simulations which are archived on the Earth System Grid Federation (ESGF) node https://esgf-node.llnl.gov/projects/cmip6/ (last access: 16 March 2022). The model source ID is UKESM1-0-LL for UKESM1 and HadGEM3-GC31-LL for HadGEM3-GC3.1. AERONET AOD data are available from https://aeronet.gsfc.nasa.gov/ (last access: 16 Mar 2022)

Author Contributions.

SW was primarily responsible for the development of the dust code and its application in UKESM1, and ran the majority of the experiments and performed the analysis. AS was scientific manager for UKESM1, coordinated the implementation of the dust code in the ESM and provided invaluable suggestions and comments throughout. YT implemented the dust settings into the UKESM1 model. MS wrote the code for dust deposition into the ocean. AY provided data and advice on deposition of dust to the ocean. ER ran the UK AMIP experiments and advised on their use. AW advised on the lai_min vegetation changes in UKESM1.

Competing Interests.

The authors declare that they have no competing interests.

https://doi.org/10.5194/acp-2022-228
Preprint. Discussion started: 1 April 2022

Acknowledgements.

This study would not have been possible without the work of many staff in the UKESM1 Core Group and the Met Office who developed the UKESM1 model and set up and ran the CMIP6 experiments. We are also grateful to all the researchers who generated the observational data we have used, including those of the AERONET community and the University of Miami Aerosol Network. We thank Claire Ryder for providing information about the FENNEC campaign.

Financial Support.

This research was supported by the Met Office Hadley Centre Climate Programme funded by BEIS and Defra (SW,AS,YT,ER,AW) as well as NERC Grant NE/N017978/1 (MS) and the EU Horizon 2020 CRESCENDO project, Grant 641816 (AY).

References

Albani, S., Mahowald, N. M., Perry, A. T., Scanza R. A., Zender, C. S., Heavens, N. G., Maggi, V., Kok, J. F.and Otto-Bleisner, B. L.: Improved dust representation in the Community Atmosphere Model, J. Adv. Model. Earth Syst., 6, 541–570, https://doi.org/10.1002/ 2013MS000279, 2014.

Alfaro, S. C. and Gomes, L.: Modeling mineral aerosol production by wind erosion: Emission intensities and aerosol size distributions in source areas, J. Geophys. Res.-Atmos., 106, 18075–18084, https://doi.org/10.1029/2000JD900339, 2001.

Archibald, A. T., O'Connor, F. M., Abraham, N. L., Archer-Nicholls, S., Chipperfield, M. P., Dalvi, M., Folberth, G. A., Dennison, F., Dhomse, S. S., Griffiths, P. T., Hardacre, C., Hewitt, A. J., Hill, R. S., Johnson, C. E., Keeble, J., Köhler, M. O., Morgenstern, O., Mulcahy, J. P., Ordóñez, C., Pope, R. J., Rumbold, S. T., Russo, M. R., Savage, N. H., Sellar, A., Stringer, M., Turnock, S. T., Wild, O., and Zeng, G.: Description and evaluation of the UKCA stratosphere–troposphere chemistry scheme (StratTrop vn 1.0) implemented in UKESM1, Geosci. Model Dev., 13, 1223–1266, https://doi.org/10.5194/gmd-13-1223-2020, 2020.

Balkanski, Y., Schulz, M., Claquin T. and Guibert S.: Reevaluation of Mineral aerosol radiative forcings suggests a better agreement with satellite and AERONET data Atmos. Chem. Phys., 7, 81–95,

Bagnold, R. A.: The Physics of Blown Sand and Desert Dunes, Methuen, New York, ISBN: 978-94-009-5682-7, 1941.

Brooks, R. H. and Corey, A. T.: Hydraulic properties of porous media ,Colorado State University,1964

Carslaw, K. S., Boucher, O., Spracklen, D. V., Mann, G. W., Rae, J. G. L., Woodward, S., and Kulmala, M.: A review of natural aerosol interactions and feedbacks within the Earth system, Atmos. Chem. Phys., 10, 1701–1737, https://doi.org/10.5194/acp-10-1701-2010, 2010.

Ramiro Checa-Garcia 1 , Yves Balkanski 1 , Samuel Albani 8 , Tommi Bergman 5 , Ken Carslaw 2 , Anne Cozic 1 , Chris Dearden 10 , Beatrice Marticorena 3 , Martine Michou 4 , Twan van Noije 5 , Pierre Nabat 4 , Fiona M. O'Connor 7 , Dirk

Olivié 6 , Joseph M. Prospero 9 , Philippe Le Sager 5 , Michael Schulz 6 , and Catherine Scott 2 Evaluation of natural aerosols in CRESCENDO Earth system models (ESMs): mineral dust Atmos. Chem. Phys., 21, 10295–10335, https://doi.org/10.5194/acp-21-10295-2021, 2021.

Collins, W. J., Bellouin, N., Doutriaux-Boucher, M., Gedney, N., Halloran, P., Hinton, T., Hughes, J., Jones, C. D., Joshi, M., Liddicoat, S., Martin, G., O'Connor, F., Rae, J., Senior, C., Sitch, S., Totterdell, I., Wiltshire, A., and Woodward, S.: Development and evaluation of an Earth-System model – HadGEM2, Geosci. Model Dev., 4, 1051–1075, https://doi.org/10.5194/gmd-4-1051-2011, 2011.

Craig, A., Valcke, S., & Coquart, L. (2017): Development and performance of a new version of the OASIS coupler, OASIS3-MCT-3.0. Geoscientific Model Development, 10 (9), 3297–3308, https://doi.org/10.5194/gmd-10-3297-2017, 2017.

Edwards, J. M. and Slingo, A.: Studies with a flexible new radiation code, part 1: Choosing a configuration for a large-scale model, Q. J. R. Meteorol. Soc., 122, 689–719, https://doi.org/10.1002/qj.49712253107, 1996.

Eyring, V., Bony, S., Meehl, G. A., Senior, C. A., Stevens, B., Stouffer, R. J., and Taylor, K. E.: Overview of the Coupled Model Intercomparison Project Phase 6 (CMIP6) experimental design and organization, Geosci. Model Dev., 9, 1937–1958, https://doi.org/10.5194/gmd-9-1937-2016, 2016.

Fécan, F., Marticorena, B. & Bergametti, G.: Parametrization of the increase of the aeolian erosion threshold wind friction velocity due to soil moisture for arid and semi-arid areas. Ann. Geophysicae 17, 149–157, https://doi.org/10.1007/s00585-999-0149-7, 1999.

Forster, P., Ramaswamy, V., Artaxo, P., Berntsen, T., Betts, R., Fahey, D. W., Haywood, J., Lean, J., Lowe, D. C., Myhre, G., Nganga, J., Prinn, R., Raga, G., Schulz, M., and Dorland, R. V.: Changes in atmospheric constituents and in radiative forcing, in: Climate Change 2007: The Physical Science Basis, Contribution of Working Group I to the Fourth Assessment Report of the Intergovernmental Panel on Climate Change, edited by: Solomon, S., Qin, D., Manning, M., Chen, Z., Marquis, M., Averyt, K. B., Tignor, M., and Miller, H. L., Cambridge Univ. Press, United Kingdom and New York, 2007.

Gillette, D. A., Environmental factors affecting dust emission by wind erosion, in: Saharan Dust, edited by Morales, C. John Wiley, New York, ISBN: 9780471996804,1979.

Ginoux, P. Effects of nonsphericity on mineral dust modeling. J. Geophys. Res.-Atmos. 108, 4052 https://doi.org/10.1029/2002JD002516, 2003.

Ginoux, P., Chin, M., Tegen, I., Prospero, J. M., Holben, B., Dubovik, O. and Lin S-J.: Sources and distributions of dust aerosols simulated with the GOCART model, J. Geophys. Res.-Atmos., 106, 20,255-20,273, https://doi.org/10.1029/2000JD000053, 2001.

Guirado, C., Cuevas, E., Cachorro, V. E., Toledano, C., Alonso-Pérez, S., Bustos, J. J., Basart, S., Romero, P. M., Camino, C., Mimouni, M., Zeudmi, L., Goloub, P., Baldasano, J. M., and de Frutos, A. M.: Aerosol characterization at the Saharan AERONET site Tamanrasset, Atmos. Chem. Phys., 14, 11753–11773, https://doi.org/10.5194/acp-14-11753-2014, 2014.

Heinold, B, Knippertz, P., Marsham, J. H., Fiedler, S., Dixon, N. S., Schepanski, K., Laurent, B.3 and Tegen, I.: The role of deep convection and nocturnal low-level jets for dust emission in summertime West Africa: Estimates from convection-permitting simulations J. Geophys. Res.-Atmos., 118, 4385–4400, https://doi.org/10.1002/jgrd.50402, 2013

Holben, B. N., Eck, T. F., Slutsker, I., Tanré, D., Buis, J. P., Setzer, A., Vermote, E., Reagan, J. A., Kaufman, Y. J., Nakajima, T., Lavenu, F., Jankowiak, I., & Smirnov, A. (1998). AERONET - A federated instrument network and data archive for aerosol characterization. In: Remote Sensing of Environment, 66(1), 1-16. https://doi.org/10.1016/S0034-4257(98)00031-5,1998.

Holben, B. N., Tanre, D., Smirnov, A., Eck, T. F., Slutsker, I., Abuhassan, N., Newcomb, W. W., Schafer, J., Chatenet, B., Lavenue, F., Kaufman, Y. J., Castle, J. V., Setzer, A., Markham, B., Clark, D., Frouin, R., Halthore, R., Karnieli, A., O'Neill, N. T., Pietras, C., Pinker, R. T., Voss, K., and Zibordi, G.: An emerging ground-based aerosol climatology: Aerosol Optical Depth from AERONET, J. Geophys. Res., 106, 12 067–12 097, https://doi.org/10.1029/2001JD900014, 2001.

Huneeus, N., Schulz, M., Balkanski, Y., Griesfeller, J., Prospero, J., Kinne, S., Bauer, S., Boucher, O., Chin, M., Dentener, F., Diehl, T., Easter, R., Fillmore, D., Ghan, S., Ginoux, P., Grini, A., Horowitz, L., Koch, D., Krol, M. C., Landing, W., Liu, X., Mahowald, N., Miller, R., Morcrette, J.-J., Myhre, G., Penner, J., Perlwitz, J., Stier, P., Takemura, T., and Zender, C. S.: Global dust model intercomparison in AeroCom phase I, Atmos. Chem. Phys., 11, 7781–7816, https://doi.org/10.5194/acp-11-7781-2011, 2011.

IGBP (2000): Global Soil Data Task (IGBP-DIS, ISO-image of CD). International Geosphere-Biosphere Program, PANGAEA, https://doi.org/10.1594/PANGAEA.869912, 2000.

Jones, C. D., Hughes, J. K., Bellouin, N., Hardiman, S. C., Jones, G. S., Knight, J., Liddicoat, S., O'Connor, F. M., Andres, R. J., Bell, C., Boo, K.-O., Bozzo, A., Butchart, N., Cadule, P., Corbin, K. D., Doutriaux-Boucher, M., Friedlingstein, P., Gornall, J., Gray, L., Halloran, P. R., Hurtt, G., Ingram, W. J., Lamarque, J.-F., Law, R. M., Meinshausen, M., Osprey, S., Palin, E. J., Parsons Chini, L., Raddatz, T., Sanderson, M. G., Sellar, A. A., Schurer, A., Valdes, P., Wood, N., Woodward, S., Yoshioka, M., and Zerroukat, M.: The HadGEM2-ES implementation of CMIP5 centennial simulations, Geosci. Model Dev., 4, 543–570, https://doi.org/10.5194/gmd-4-543-2011, 2011.

Knippertz, P., and Todd, M. C.: Mineral dust aerosols over the Sahara: Meteorological controls on emission and transport and implications for modeling, Rev. Geophys., 50, RG1007, https://doi.org/10.1029/2011RG000362, 2012.

Kohfeld, K., and Harrison, S. P.: DIRTMAP: The geologic record of dust, Earth Sci. Rev., 54, 81 – 114, https://doi.org/10.1016/S0012-8252(01)00042-3, 2001

Kok, J. F., Mahowald, N. M., Fratini, G., Gillies, J. A., Ishizuka, M., Leys, J. F., Mikami, M., Park, M.-S., Park, S.-U., Van Pelt, R. S., and Zobeck, T. M.: An improved dust emission model – Part 1: Model description and comparison against measurements, Atmos. Chem. Phys., 14, 13023–13041, https://doi.org/10.5194/acp-14-13023-2014, 2014.

Kok, J. F., Ridley, D. A., Zhou, Q., Miller, R. L., Zhao, C., Heald, C. L., Ward, D. S., Albani, S., and Haustein, K.: Smaller desert dust cooling effect estimated from analy- sis of dust size and abundance, Nat. Geosci., 10, 274–278, https://doi.org/10.1038/Ngeo2912, 2017.

Kok, J.F., Ward, D.S., Mahowald, N.M. and Evan A. T.: Global and regional importance of the direct dust-climate feedback,. Nat. Commun. 9, 241, https://doi.org/10.1038/s41467-017-02620-y, 2018.

Citation:

Kuhlbrodt, T., Jones, C. G., Sellar, A., Storkey, D., Blockley, E., Stringer, M. and Walton, J.: The low-resolution version of HadGEM3 GC3.1: Development and evaluation for global climate. J. Adv. Model. Earth Sy., 10, 2865–2888. https://doi.org/10.1029/2018MS0013, 2018.

Levy, R. C., Mattoo, S., Munchak, L. A., Remer, L. A., Sayer, A. M., Patadia, F., and Hsu, N. C.: The Collection 6 MODIS aerosol products over land and ocean, Atmos. Meas. Tech., 6, 2989–3034, https://doi.org/10.5194/amt-6-2989-2013, 2013.

Loveland, T. R., Reed, B. C., Ohlen, D. O., Brown, J. F., Zhu, Z., Yang, L. and Merchant, J. W.: Development of a global land cover characteristics database and IGBP DISCover from 1 km AVHRR data, Int. J. Remote Sens., https://doi.org/10.1080/014311600210191, 2000.

Mahowald, N. M., Kohfeld, K., Hansson, M., Balkanski, Y., Harrison, S. P., Prentice, I. C., Schulz, M., and Rodhe, H.: Dust sources and deposition during the last glacial maximum and current climate: A comparison of model results with paleodata from ice cores and marine sediments, J. Geophys. Res.-Atmos., 104, 15895–15916, https://doi.org/10.1029/1999JD900084, 1999.

Mahowald, N. M., Muhs, D. R., Levis, S., Rasch, P. J., Yoshioka, M., Zender, C. S., and Luo, C.: Change in atmospheric mineral aerosols in response to climate: Last glacial period, preindustrial, modern, and doubled carbon dioxide climates, J. Geophys. Res.-Atmos., 111, D10202, https://doi.org/10.1029/2005JD006653, 2006.

Mahowald, N. M., Engelstaedter, S., Luo, C., Sealy, A., Artaxo, P., Benitez-Nelson, C., Bonnet, S., Chen, Y., Chuang, P. Y., Cohen, D. D., Dulac, F., Herut, B., Johansen, A. M., Kubilay, N., Losno, R., Maenhaut, W., Paytan, A., Prospero, J. M., Shank, L. M., Siefert, R. L.,; Atmospheric iron deposition: global distribution, variability, and human perturbations, Ann. Rev. Mar. Sci., 1, 245-78, https://doi.org/ 10.1146/annurev.marine.010908.163727, 2009.

Marsham, J. H., Knippertz, P., Dixon, N. S., Parker, D. J. and Lister G. M. S., The importance of the representation of deep convection for modeled dust-generating winds over West Africa during summer, Geophys. Res. Lett., 38, L16803, https://doi.org/10.1029/2011GL048368, 2011.

Marticorena, B., and Bergametti G., Modeling the atmospheric dust cycle: 1. Design of a soil-derived dust emission scheme, J. Geophys. Res., 100, 16,415 – 16,430. https://doi.org/10.1029/95JD00690, 1995.

Marticorena, B., Chatenet, B., Rajot, J. L., Traoré, S., Coulibaly, M., Diallo, A., Koné, I., Maman, A., NDiaye, T., and Zakou, A.: Temporal variability of mineral dust concentrations over West Africa: analyses of a pluriannual monitoring from the AMMA Sahelian Dust Transect, Atmos. Chem. Phys., 10, 8899–8915, https://doi.org/10.5194/acp-10-8899-2010, 2010.

Marticorena, B., Chatenet, B., Rajot, J. L., Bergametti, G., Deroubaix, A., Vincent, J., Kouoi, A., Schmechtig, C., Coulibaly, M., Diallo, A., Koné, I., Maman, A., NDiaye, T., and Zakou, A.: Mineral dust over west and central Sahel: Seasonal patterns of dry and wet deposition fluxes from a pluriannual sampling (2006–2012), J. Geophys. Res.-Atmos., 122, 1338–1364, https://doi.org/10.1002/2016JD025995, 2017

Miller, R. L., Cakmur, R. V., Perlwitz, J., Geogdzhayev, I. V., Ginoux, P., Koch, D., Kohfeld, K. E., Prigent, C., Ruedy, R., Schmidt, G. A., and Tegen, I.: Mineral dust aerosols in the NASA Goddard Institute for Space Sciences ModelE atmospheric general circulation model, J. Geophys. Res.-Atmos., 111, D06208, https://doi.org/10.1029/2005JD005796, 2006

Moss, R. H., Edmonds, J. A., Hibbard, K. A., Manning, M. R., Rose, S. K., Vuuren, D. P. van, Carter, T. R., Emori, S., Kainuma, M., Kram, T., Meehl, G. A., Mitchell, J. F. B., Nakicenovic, N., Riahi, K., Smith, S. J., Stouffer, R. J., Thomson, A. M., Weyant, J. P., & Wilbanks, T. J.: The next generation of scenarios for climate change research and assessment. Nature, 463, 747–756. https://doi.org/10.1038/nature08823, 2010.

Mulcahy, J. P., Johnson, C., Jones, C. G., Povey, A. C., Scott, C. E., Sellar, A., Turnock, S. T., Woodhouse, M. T., Abraham, N. L., Andrews, M. B., Bellouin, N., Browse, J., Carslaw, K. S., Dalvi, M., Folberth, G. A., Glover, M., Grosvenor, D. P., Hardacre, C., Hill, R., Johnson, B., Jones, A., Kipling, Z., Mann, G., Mollard, J., O'Connor, F. M., Palmiéri, J., Reddington, C., Rumbold, S. T., Richardson, M., Schutgens, N. A. J., Stier, P., Stringer, M., Tang, Y., Walton, J., Woodward, S., and Yool, A.: Description and evaluation of aerosol in UKESM1 and HadGEM3-GC3.1 CMIP6 historical simulations, Geosci. Model Dev., 13, 6383–6423, https://doi.org/10.5194/gmd-13-6383-2020, 2020

Mulcahy, J. P., Jones, C., Rumbold, S., Kuhlbrodt, T., Dittus, A. J., Blockley, E. W., Yool, A., Walton, J., Hardacre, C., Andrews, T., Bodas-Salcedo, A., Stringer, M., de Mora L., Harris, P., Hill, R., Kelley, D., Robertson, E and Y. Tang: Development and evaluation of an updated configuration of UKESM1: UKESM1.1, JAMES, 2022, submitted.

Nachtergaele, F., van Velthuizen, H., Verelst, L., Batjes, N., Dijkshoorn, K., van Engelen, V., Fischer, G., Jones, A., Montanarella, L., Petri,M., Prieler, S., Teixeira, E., Wiberg, D., and Shi, X.: Harmonized World Soil Database (version 1.0), FAO, Rome, Italy and IIASA,Laxenburg, Austria, 2008

Prospero, J. M., Landing, W. M., and Schulz, M.: African dust deposition to Florida: Temporal and spatial variability and comparisons to models, J. Geophys. Res., 115, D13304, https://doi.org/10.1029/2009JD012773, 2010.

Riahi, K., Van Vuuren, D. P., Kriegler, E., Edmonds, J., O'neill, B. C., Fujimori, S., Bauer, N., Calvin, K., Dellink, R., Fricko, O., Lutz, W., Popp, A., Cuaresma, J. C., Samir K. C., Leimbach, M., Jiang, L., Kram, T., Rao, S., Emmerling, J., Ebi, K., Hasegawa, T., Havlik, P., Humpenöder, F., Da Silva, L. A., Smith, S., Stehfest, E., Bosetti, V., Eom, J., Gernaat, D., Masui, T., Rogelj, J., Strefler, J., Drouet, L., Krey, V., Luderer, G., Harmsen, M., Takahashi, K., Baumstark, L., Doelman, J. C., Kainuma, M., Klimont, Z., Marangoni, G., Lotze-Campen, H., Obersteiner, M., Tabeau, A. and Tavoni M.: The Shared Socioeconomic Pathways and their energy, land use, and greenhouse gas emissions implications: An overview, Global Environmental Change, 42, 153-168, https://doi.org/10.1016/j.gloenvcha.2016.05.009, 2017.

Ridley, J. K., Blockley, E. W., Keen, A. B., Rae, J. G. L., West, A. E., and Schroeder, D.: The sea ice model component of HadGEM3-GC3.1, Geosci. Model Dev., 11, 713–723, https://doi.org/10.5194/gmd-11-713-2018, 2018.

Ryder, C. L., Highwood, E. J., Rosenberg, P. D., Trembath, J., Brooke, J. K., Bart, M., Dean, A., Crosier, J., Dorsey, J., Brindley, H., Banks, J., Marsham, J. H., McQuaid, J. B., Sodemann, H., and Washington, R.: Optical properties of Saharan dust aerosol and contribution from the coarse mode as measured during the Fennec 2011 aircraft campaign, Atmos. Chem. Phys., 13, 303–325, https://doi.org/10.5194/acp-13-303-2013, 2013.

Ryder, C. L., Highwood, E. J., Walser, A., Seibert, P., Philipp, A., and Weinzierl, B.: Coarse and giant particles are ubiquitous in Saharan dust export regions and are radiatively significant over the Sahara, Atmos. Chem. Phys., 19, 15353–15376, https://doi.org/10.5194/acp-19-15353-2019, 2019

Scanza, R. A., Mahowald, N., Ghan, S., Zender, C. S., Kok, J. F., Liu, X., Zhang, Y., and Albani, S.: Modeling dust as component minerals in the Community Atmosphere Model: development of framework and impact on radiative forcing, Atmos. Chem. Phys., 15, 537–561, https://doi.org/10.5194/acp-15-537-2015, 2015.

Sellar, A. A., Jones, C. G., Mulcahy, J. P., Tang, Y., Yool, A., Wiltshire, A., O'Connor, F. M., Stringer, M., Hill, R., Palmieri, J., Woodward, S., de Mora, L., Kuhlbrodt, T., Rumbold, S. T., Kelley, D. I., Ellis, R., Johnson, C. E., Walton, J., Abraham, N. L., Andrews, M. B., Andrews, T., Archibald, A. T., Berthou, S., Burke, E., Blockley, E., Carslaw, K., Dalvi, M., Edwards, J., Folberth, G. A., Gedney, N., Griffiths, P. T.,Harper, A. B., Hendry, M. A., Hewitt, A. J., Johnson, B., Jones, A., Jones, C. D., Keeble, J., Liddicoat, S., Morgenstern, O. , Parker, R. J., Predoi, V., Robertson, E., Siahaan, A., Smith, R. S., Swaminathan, R., Woodhouse, M. T., Zeng, G., and Zerroukat, M.: UKESM1: Description and Evaluation of the U.K. Earth System Model, J. Adv. Model. Earth Sy., 11, 4513–4558, https://doi.org/10.1029/2019MS001739, 2019.

Sellar, A. A., Walton, J., Jones, C. G., Wood, R., Abraham, N. L., Andrejczuk, M., Andrews, M. B., Andrews, T., Archibald, A. T., de Mora, L., Dyson, H., Elkington, M., Ellis, R., Florek, P., Good, P., Gohar, L., Haddad, S., Hardiman, S. C., Hogan, E., Iwi, A., Jones, C. D., Johnson, B., Kelley, D. I., Kettleborough, J., Knight, J. R., Köhler, M. O., Kuhlbrodt, T., Liddicoat, S., Linova-Pavlova, I., Mizielinski, M. S., Morgenstern, O., Mulcahy, J., Neininger, E., O'Connor, F. M., Petrie, R., Ridley, J., Rioual, J. C., Roberts, M., Robertson, E., Rumbold, S., Seddon, J., Shepherd, H., Shim, S., Stephens, A., Teixiera, J. C., Tang, Y., Williams, J., Wiltshire, A., and Griffiths, P. T.: Implementation of U. K. Earth System Models for CMIP6, J. Adv. Model. Earth Sy., 12, https://doi.org/10.1029/2019MS001946, 2020.

Sokolik, I. N., and Toon, O. B.: Incorporation of mineralogical composition into models of the radiative properties of mineral aerosol from UV to IR wavelengths, J. Geophys. Res., 104, 9423-9444, https://doi.org/10.1029/1998JD200048, 1999.

Storkey, D., Blaker, A. T., Mathiot, P., Megann, A., Aksenov, Y., Blockley, E. W., Calvert, D., Graham, T., Hewitt, H. T., Hyder, P., Kuhlbrodt, T., Rae, J. G. L., and Sinha, B.: UK Global Ocean GO6 and GO7: a traceable hierarchy of model resolutions, Geosci. Model Dev., 11, 3187 –3213, https://doi.org/10.5194/gmd-11-3187-2018, 2018

Tegen, I., and Fung, I.: Modeling of mineral dust in the atmosphere: Sources, transport, and optical thickness, J. Geophys. Res., 99, 22,897-22,914, https://doi.org/10.1029/94JD01928, 1994

Tegen, I., Harrison, S. P., Kohfeld, K., Prentice, I. C., Coe, M., and Heimann, M.: Impact of vegetation and preferential source areas on global dust aerosol: Results from a model study, J. Geophys. Res.-Atmos., 107, AAC 14-1–AAC 14-27, https://doi.org/10.1029/2001JD000963, 2002.

Tilmes, S., Lamarque, J., Emmons, L. K., Kinnison, D. E., Marsh, D., Garcia, R. R., Smith, A. K., Neely, R. R., Conley, A., Vitt, F., Martin, M. V., Tanimoto, H., Simpson, I., Blake, D. R. and Blake, N.: Representation of the Community Earth

System Model (CESM1) CAM4-chem within the Chemistry-Climate Model Initiative (CCMI), Geosci. Model Dev., 9, 1853–1890, https://doi.org/10.5194/gmd-9-1853-2016, 2016

Textor, C., Schulz, M., Guibert, S., Kinne, S., Balkanski, Y., Bauer, S., Berntsen, T., Berglen, T., Boucher, O., Chin, M., Dentener, F., Diehl, T., Easter, R., Feichter, H., Fillmore, D., Ghan, S., Ginoux, P., Gong, S., Grini, A., Hendricks, J., Horowitz, L., Huang, P., Isaksen, I., Iversen, I., Kloster, S., Koch, D., Kirkevåg, A., Kristjansson, J. E., Krol, M., Lauer, A., Lamarque, J. F., Liu, X., Montanaro, V., Myhre, G., Penner, J., Pitari, G., Reddy, S., Seland, Ø., Stier, P., Takemura, T., and Tie, X.: Analysis and quantification of the diversities of aerosol life cycles within AeroCom, Atmos. Chem. Phys., 6, 1777–1813, https://doi.org/10.5194/acp-6-1777-2006, 2006.

Todd, M. C., Washington, R., Martins, J. V., Dubovik, O., Lizcano, G., M'Bainayel, S., and Engelstaedter, S.: Mineral dust emission from the Bodel ´ e Depression, Northern Chad, during BoDEx 2005, J. Geophys. Res., 112, D06207, https://doi.org/10.1029/2006JD007170, 2007.

Todd, M. C., Washington, R., Raghavan, S., Lizcano, G., and Knippertz, P.: Regional model simulations of the Bodele low-level jet of northern Chad during the Bodele Dust Experiment (BoDEx 2005), J. Climate, 21, 995–1012, https://doi.org/10.1175/2007jcli1766.1, 2008.

van Vuuren, D. P., Edmonds, J., Kainuma, M., Riahi, K., Thomson, A., Hibbard, K., Hurtt, G. C., Kram, T., Krey, V., Lamarque, J.-F., Masui, T., Meinshausen, M., Nakicenovic, N., Smith, S. J., and Rose, S. K.: The representative concentration pathways: an overview, Climatic Change, 109, 5–31, https://doi.org/10.1007/s10584-011-0148-z, 2011.

Walters, D., Baran, A. J., Boutle, I., Brooks, M., Earnshaw, P., Edwards, J., Furtado, K., Hill, P., Lock, A., Manners, J., Morcrette, C., Mulcahy, J., Sanchez, C., Smith, C., Stratton, R., Tennant, W., Tomassini, L., Van Weverberg, K., Vosper, S., Willett, M., Browse, J., Bushell, A., Carslaw, K., Dalvi, M., Essery, R., Gedney, N., Hardiman, S., Johnson, B., Johnson, C., Jones, A., Jones, C., Mann, G., Milton, S., Rumbold, H., Sellar, A., Ujiie, M., Whitall, M., Williams, K., and Zerroukat, M.: The Met Office Unified Model Global Atmosphere 7.0/7.1 and JULES Global Land 7.0 configurations, Geosci. Model Dev., 12, 1909–1963, https://doi.org/10.5194/gmd-12-1909-2019, 2019.

Watanabe, S., Hajima, T., Sudo, K., Nagashima, T., Takemura, T., Okajima, H., Nozawa, T., Kawase, H., Abe, M., Yokohata, T., Ise, T., Sato, H., Kato, E., Takata, K., Emori, S., and Kawamiya, M.: MIROC-ESM 2010: model description and basic results of CMIP5-20c3m experiments, Geosci. Model Dev., 4, 845–872, https://doi.org/10.5194/gmd-4-845-2011, 2011.

Williams, K. D., Copsey, D., Blockley, E. W., Bodas-Salcedo, A., Calvert, D., Comer, R., Davis, P., Graham, T., Hewitt, H. T., Hill, R., Hyder, P., Ineson, S., Johns, T. C., Keen, A. B., Lee, R. W., Megann, A., Milton, S. F., Rae, J. G. L., Roberts, M. J., Scaife, A. A., Schiemann, R., Storkey, D., Thorpe, L., Watterson, I. G., Walters, D. N., West, A., Wood, R. A., Woollings, T., and Xavier, P. K.: The Met Office Global Coupled Model 3.0 and 3.1 (GC3.0 and GC3.1) configurations, J. Adv. Model Earth Syst., 10, 357–380, https://doi.org/10.1002/2017MS001115, 2018.

Woodage, M. J. and Woodward, S.: U.K. HiGEM: Impacts of Desert Dust Radiative Forcing in a High-Resolution Atmospheric GCM, J. Clim. 27, 5907-5928, https://doi.org/10.1175/JCLI-D-13-00556.1, 2014

https://doi.org/10.5194/acp-2022-228
Preprint. Discussion started: 1 April 2022


Atmospheric Chemistry and Physics Discussions

Woodward, S.: Modeling the atmospheric life cycle and radiative impact of mineral dust in the Hadley Centre climate model, J. Geophys. Res., 106, 18155–18166, https://doi.org/10.1029/2000JD900795, 2001.

Yool, A., Popova, E. E., and Anderson, T. R.: MEDUSA-2.0: an intermediate complexity biogeochemical model of the marine carbon cycle for climate change and ocean acidification studies, Geosci. Model Dev., 6, 1767–1811, https://doi.org/10.5194/gmd-6-1767-2013, 2013.

Zender, C. S., Bian, H. and Newman, D.: Mineral Dust Entrainment and Deposition (DEAD) model: Description and 1990s dust climatology, J. Geophys. Res. D Atmos., https://doi.org/10.1029/2002jd002775, 2003.